PART I The methods of nuclear physics

1 Introduction

1.1 General survey

It is customary to regard nuclear physics as the field of study that includes the structure of atomic nuclei, the reactions that take place between them, and the techniques, both experimental and theoretical, that shed light on these subjects. Rigid adherence to such limits would, however, exclude much that is both exciting and informative. The nucleus entered physics as a necessary component of the atomic model and nuclear effects in spectroscopy and solid state physics now provide not only elegant methods for determination of nuclear properties but also convincing demonstrations of the powers of quantum mechanics. Equally, those particles sometimes described as elementary or fundamental, although first recognized in the cosmic radiation, soon assumed a role of importance in nuclear problems, especially in the understanding of the forces between neutrons and protons. Advances in the study of particles, or sub-nuclear physics, besides leading to the discovery of new and previously unsuspected physical laws, have frequently stimulated back-reference to complex nuclei for the testing of some new hypothesis or some presumed symmetry. On a less fundamental but socially more significant plane, the exciting problems of astrophysical energy generation and the basic technology of terrestrial power sources relate directly to nuclear structure and nuclear dynamics.

Nuclear physics, therefore, is not a self-sufficient and not an isolated subject. Nor is it strictly a modern subject, since it derives from Becquerel's experiments of 1896, and from Rutherford's wholly classical scattering studies of 1911. Rather, it is an essential ingredient in our understanding of the nature of matter at a level deeper than that of the electronic structure of atoms, molecules and solids but not so deep as that of the particle structure of the proton and neutron.

1.2 Collisions between particles

Collision phenomena provided the original evidence for the hypothesis of the nucleus and have also offered, from the earliest days, powerful methods of studying both nuclear forces and nuclear structure. Although a wave-mechanical treatment is usually necessary for the detailed interpretation of collision experiments, many problems of interest only involve de Broglie wavelengths that are small compared with sizes or geometrical constraints, and classical trajectory calculations can then be made. In all cases it is useful to distinguish between the *kinematic* features of the collision, which are governed by the laws of conservation of energy and of linear and angular momentum, and the *dynamical* features, e.g. the frequency of occurrence of events of a given type, which are determined by the energy available in the collision, by the nature of the forces between the interacting objects and by their internal structure.

1.2.1 *Elastic scattering (non-relativistic)*

A collision between two particles is *elastic* if the particles of the final state (f) are identical with those of the initial state (i). 'Identical' means that in both states i and f the particles are in their ground state, i.e. without internal excitation energy. The principle of conservation of energy then requires that the total kinetic energy is conserved between initial and final states, i.e. $T_i = T_f$.

Figure 1.1 defines kinematic parameters for such a collision in

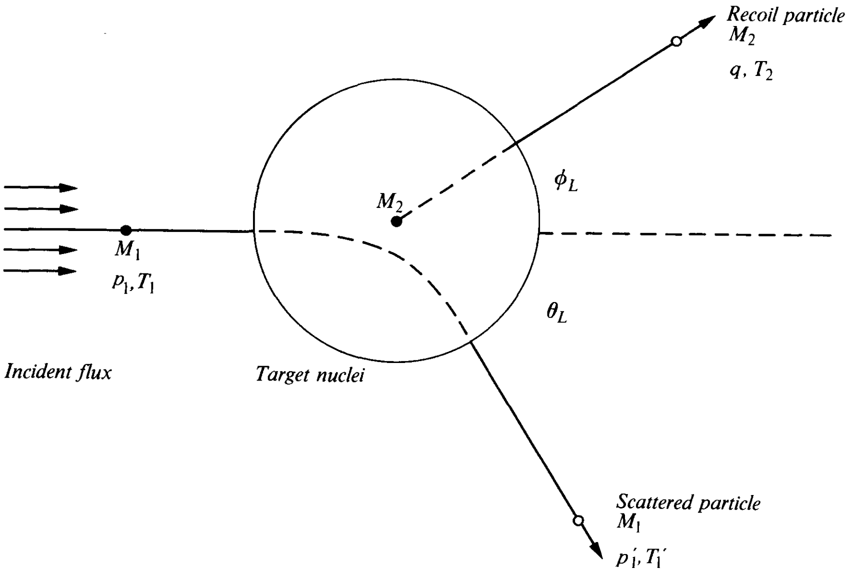

Fig. 1.1 Elastic collision between particles, laboratory coordinates. The circle indicates schematically that within the range of nuclear forces, details of the collision may not be known. The conservation laws for energy and momentum, however, determine the kinematics of the process.

which particles of mass M_1, e.g. from an accelerator, strike particles of mass M_2, equal to nM_1, say. There is a certain region of interaction in which the detailed behaviour of the system is usually not known but when the separation of the particles exceeds the range of their mutual force, some predictions can be made. These follow from the conservation laws for linear momentum and energy, namely

$$\boldsymbol{p}_1 = \boldsymbol{p}_1' + \boldsymbol{q} \tag{1.1}$$

and, for an elastic collision,

$$T_1 = T_1' + T_2 \tag{1.2}$$

together with the non-relativistic relation between momentum and energy

$$p^2 = 2MT \tag{1.3}$$

where p is the absolute magnitude of the vector $\boldsymbol{p}$, i.e. $|\boldsymbol{p}|$. Useful predictions are, referring to Fig. 1.1:

(i) *Angle* $(\theta_L + \phi_L)$ *between particles after collision.* This may be obtained by taking the scalar product of equation (1.1) with itself since the required angle is just that between the two vectors on the right-hand side. The result is

$$p_1^2 = (p_1')^2 + q^2 + 2p_1'q \cos(\theta_L + \phi_L)$$

Substituting for the squared momenta and using $n = M_2/M_1$ we find

$$T_1 = T_1'{}^{-}T_2 + p_1'q \cos(\theta_L + \phi_L)/M_1 \tag{1.4}$$

For equal masses, $n = 1$, and from equation (1.2) it follows that $\cos(\theta_L + \phi_L) = 0$, i.e. $\theta_L + \phi_L = \pi/2$. Similarly, for unequal masses with $n > 1$, $(\theta_L + \phi_L) > \pi/2$ while with $n < 1$, $(\theta_L + \phi_L) < \pi/2$. These are the cases of a particle striking a heavier and lighter target respectively.

(ii) *Energy of the scattered particle* T_1' *in terms of the scattering angle* θ_L. In this case we are interested in the angle between $\boldsymbol{p}_1$ and $\boldsymbol{p}_1'$, so equation (1.1) is rearranged before forming a scalar product to read

$$\boldsymbol{q} = \boldsymbol{p}_1 - \boldsymbol{p}_1'$$

whence

$$q^2 = p_1^2 + p_1'^2 - 2p_1p_1' \cos\theta_L$$

Converting to energies

$$nT_2 = T_1 + T_1' - 2(T_1T_1')^{1/2} \cos\theta_L$$

where $T_1^{1/2}$ and $T_1'^{1/2}$ are both positive since p_1 and p_1' are positive. Eliminating T_2 by using the energy equation and rearranging

$$2(T_1'/T_1)^{1/2} \cos\theta_L = (T_1'/T_1)(1 + n) - (1 - n)$$

whence

$$(T_1'/T_1)^{1/2} = \cos\theta_L[1 \pm (1-(1-n^2)/\cos^2\theta_L)^{1/2}]/(1+n) \qquad (1.5)$$

For equal masses $n=1$ and $T_1' = T_1\cos^2\theta_L$. At $\theta_L = \pi/2, \phi_L = 0$, and the incident energy is wholly transferred to the struck particle. The incident particle cannot be scattered backwards ($\theta_L > \pi/2$). A familiar example in nuclear physics is the scattering of neutrons by protons. For unequal masses, if $n>1$ the sign $\pm$ in equation (1.5) must be chosen so that $(T_1'/T_1)^{1/2} = p_1'/p_1$ is positive. There is then a *single* value T_1' for each θ_L and any value of θ_L is possible. This is seen in the nuclear scattering of β-particles passing through matter. The maximum kinetic energy transfer to the target nucleus $T_1 - T_1'$ is found from equation (1.5) to be $4T_1/n = 4T_1M_1/M_2$ for large n.

In the case of unequal masses when $n<1$, as in the collision of an α-particle with an electron, equation (1.5) requires that $\cos^2\theta_L \geqslant 1-n^2$ so that $\sin\theta_L \leqslant n$, i.e. the scattering angle is always less than $\pi/2$ and tends to zero for $n \ll 1$, so that the heavy particle continues essentially undeviated. In this case the maximum energy conveyed to the target particle is approximately $4nT_1 = 4T_1M_2/M_1$. The alternative signs in equation (1.5) now allow *two* values of T_1' for each allowed θ_L, except $\theta_L = \sin^{-1} n$. This is best understood by reference to the centre-of-mass coordinate system (Sect. 1.2.3).

(iii) *Momentum transfer* $\boldsymbol{q}$ *to* M_2. In a similar way (see Ex. 1.1) it can be shown that

$$q = |\boldsymbol{q}| = |\boldsymbol{p}_1|(2n/(1+n))\cos\phi_L \qquad (1.6)$$

In later chapters, this important quantity will often appear in the form $\boldsymbol{q} = \boldsymbol{q}_i - \boldsymbol{q}_f$ where $\boldsymbol{q}_i$ and $\boldsymbol{q}_f$ are the momentum vectors of a particle before and after scattering.

1.2.2 *Inelastic reactions (non-relativistic)*

A collision between two particles is *inelastic* if the particles of the final state (f) are different from those of the initial state (i). They may be of a different kind, or in different states of excitation. In such a collision, linear momentum is still conserved but *kinetic* energy is not. The conservation law for energy between states i and f now reads

$$T_i + Q = T_f \qquad (1.7)$$

where T_i and T_f are the total kinetic energies in states i, f, and Q is a constant for a given reaction; equation (1.7) defines the *Q-value* as the difference between the total kinetic energies in the final and initial states. For elastic scattering, $Q=0$.

Typical inelastic *reactions* are the first example of artificial transmutation, discovered by Rutherford in 1919 and later photographed by Blackett in a cloud chamber:

$$^{14}N+{}^{4}He \rightarrow {}^{17}O+{}^{1}H \quad (Q=-1{\cdot}19\,\text{MeV}) \tag{1.8a}$$

and the first example of transmutation by accelerated particles (Cockcroft and Walton 1932):

$$^{7}Li+{}^{1}H \rightarrow 2\,{}^{4}He \quad (Q=+17{\cdot}35\,\text{MeV}) \tag{1.8b}$$

These reactions are often abbreviated in the form $^{14}N(\alpha, p)^{17}$ and $^{7}Li(p, \alpha)\alpha$ using the special symbols for the light particles.

Inelastic *scattering*, as distinct from an inelastic reaction, does not alter the basic nature of the reacting particles but excites energy levels of one or both, e.g.

$$^{27}Al+p \rightarrow {}^{27}Al^{*}+p' \quad (Q=-0{\cdot}84, -1{\cdot}01, \ldots \text{MeV}) \tag{1.9}$$

This reaction is abbreviated $^{27}Al(p, p')^{27}Al^{*}$ where the symbol $^{27}Al^{*}$ indicates an aluminium nucleus in an excited state and p′ indicates a proton group with an energy less than the incident energy because of transfer to the particular excited state. Figure 1.2*a* shows the lowest few levels of the ^{27}Al nucleus and Fig. 1.2*b* represents the observed energy spectrum of the inelastic proton groups $p_0, p_1', \ldots, p_4'$, of which p_0 relates to the *ground state* ^{27}Al and is the *elastic* group that is always present. The study of level schemes by inelastic scattering is a basic technique of nuclear spectroscopy. A complementary technique is to measure the energies of the γ-rays emitted when the excited nucleus $^{27}Al^{*}$ returns to its ground state ^{27}Al (Fig. 1.2*c*). The discrete energies found may be correlated with the levels as shown in Fig. 1.2*a*. Together, these two studies present a complete analogy with the Franck–Hertz experiment of atomic physics.

The origin of a finite Q-value in processes (1.8a) and (1.8b) cannot be understood classically, but is immediately clear when relativistic mechanics is used (Sect. 1.2.4) because of the mass–energy relation $E=mc^2$. For the present we simply note that inelastic collisions can be treated in the same way as elastic processes using the equations, in the notation of Fig. 1.3:

$$\left.\begin{aligned} \boldsymbol{p}_1 &= \boldsymbol{p}_3+\boldsymbol{p}_4 \\ T_1+Q &= T_3+T_4 \\ p^2 &= 2MT \end{aligned}\right\} \tag{1.10}$$

The modified energy equation makes calculations more complicated, but the methods are the same as for elastic processes. Thus, we can show that the kinetic energy T_3 of the product particle M_3 is related to the scattering angle θ_{3L} by the equation

$$(M_3+M_4)T_3-2(M_1M_3T_1T_3)^{1/2}\cos\theta_{3L}=(M_4-M_1)T_1+M_4Q \tag{1.11}$$

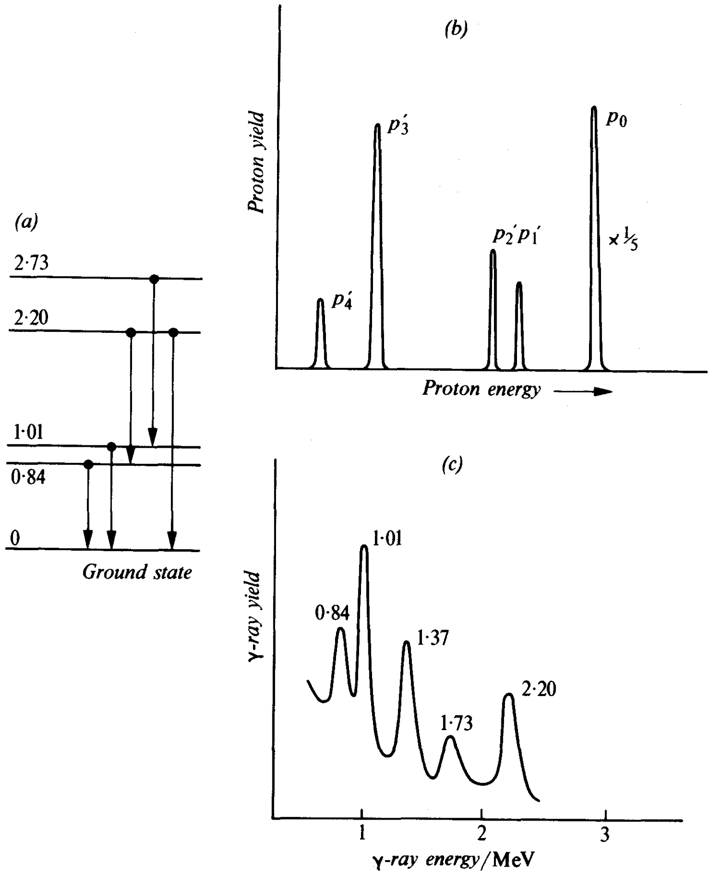

Fig. 1.2 (*a*) Levels of ^{27}Al nucleus, with excitation indicated in MeV. (*b*) Spectrum of inelastically scattered protons in the reaction $Al^{27}(p, p')^{27}Al^*$. (*c*) Spectrum of de-excitation γ-radiation following inelastic scattering. The radiative transitions are shown on the level diagram (*a*).

which again predicts a double-valued energy at a given angle under certain conditions (see Ex. 1.4 and Sect. 1.2.3) but in most cases determines a unique energy T_3 at a given θ_{3L}. Observation of the spectrum of M_3 then leads to a series of Q-values corresponding with the excited states of M_4 assuming that M_3 itself is unexcited.

Equations (1.10) show that an exothermic reaction (Q + ve) can occur even when T_1 is zero, assuming that the reacting nuclei can approach sufficiently close. For endothermic reactions (Q − ve), however, the kinetic energy of the incident particle must exceed a certain threshold energy in order to permit momentum conservation. It can be shown (see Ex. 1.5 and Sect. 1.2.3) that the threshold

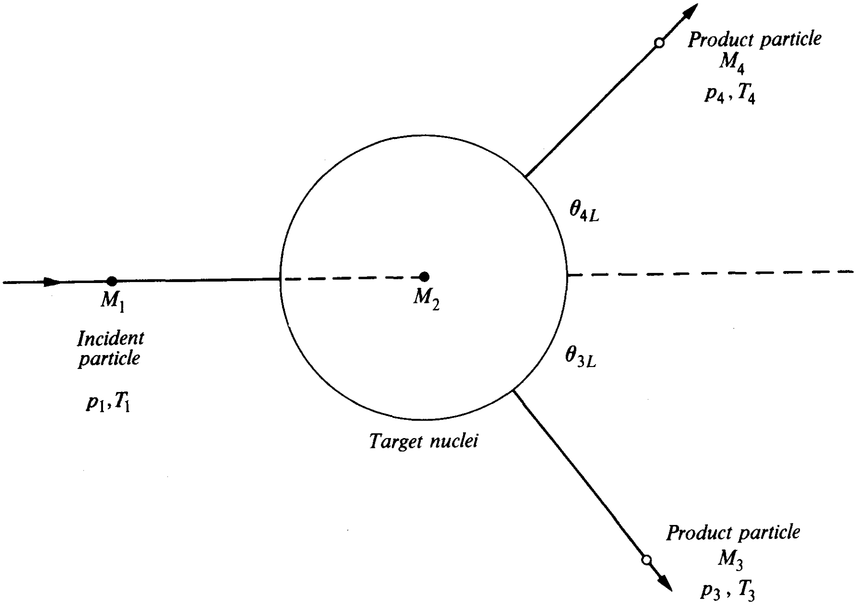

Fig. 1.3 Inelastic collision between particles, laboratory coordinates. The products M_3 and M_4 may be the same as M_1 and M_2 but with some excitation energy; the collision is then described as an *inelastic scattering process.*

energy is $T_1 = |Q|(M_1 + M_2)/M_2$ with the assumption that for kinematic calculations we may write for masses the classical equality $M_1 + M_2 = M_3 + M_4$. The relativistic calculation (eqn. (1.26)) gives a slightly different result because mass is not conserved.

1.2.3 Centre-of-mass system (non-relativistic)

In the classical two-body problem, with no external forces, it is possible to describe the motion by two completely separate equations, one of which defines the motion of the mass centre, while the other gives the *relative* motion of the two particles. *Relative motion* means the variation with time of the distance between the particles. A similar separation may be made when the interaction must be described by Schrödinger's wave equation. The mass centre moves with the same constant velocity before and after the interaction, whatever the nature of the forces between the particles; these forces affect the relative motion only (Ref. 1.2*a*, Chs. 18 and 19). Thus, the complete motion is the resultant of the centre-of-mass motion and the relative motion, and since collisions are usually studied with the object of learning about the forces between the particles, the first step in comparing observation with theory is to 'subtract-off' the irrelevant motion of the mass centre. That is, one must learn how to transform scattering angles and energies from the laboratory system, which is usually the rest-system of one of the initial-state particles, to those values which would have been obtained had the experiment been carried out in a frame of reference in which the mass centre was stationary. A Galilean transformation is the appropriate one for a non-relativistic treatment.

In the centre-of-mass (c.m.) system the momenta of the particles are equal and opposite both before and after the collision, and for this reason this system is often called the 'zero momentum system'. Only in the special case of a 'storage ring' collision between oppositely moving particles of equal mass and equal energy are the laboratory and c.m. systems identical, and each is of zero momentum. In the more usual case, where the target particle is intially stationary in the laboratory (see Fig. 1.1), the velocity of the centre-of-mass in the laboratory system is given by

$$v_c = (p_1/M_1)M_1/(M_1+M_2) = p_1/(M_1+M_2) \tag{1.12}$$

and the equal and opposite momenta of particles 1 and 2 in the c.m. system are given numerically by

$$p_c = p_1M_2/(M_1+M_2) = p_1n/(1+n)$$

where n $(=M_2/M_1)$ is easily seen to be equal to the ratio of the velocity of M_1 in the c.m. system to v_c, the velocity of the c.m. in the laboratory.

The c.m. momentum p_c is the momentum of a particle of the *reduced mass*

$$\mu = M_1M_2/(M_1+M_2) \tag{1.13}$$

moving with the incident particle velocity (p_1/M_1). The corresponding c.m. wavenumber is

$$k = 1/\lambda\!\!\!^{-} = (\mu/\hbar)(p_1/M_1) \tag{1.14}$$

The c.m. kinetic energies follow from the non-relativistic relation (1.3); thus M_1 has energy $p_c^2/2M_1$, M_2 has $p_c^2/2M_2$ and the total kinetic energy is the sum of these, namely $\frac{1}{2}\mu(p_1/M_1)^2$, which is less than the incident energy $p_1^2/2M_1$ by an amount $\frac{1}{2}(M_1+M_2)v_c^2$. This is the energy associated with the motion of the mass centre.

The relations obtained so far relate to conditions before the collision. Afterwards, if the collision is *elastic* (Fig. 1.4*a*) kinetic energies and absolute values of momenta are unchanged in the c.m. system but the momenta are differently directed. Only one scattering angle is needed to describe the collision. To return to the laboratory system, the c.m. velocity must be restored and the corresponding momentum changes are shown in Fig. 1.4*b*. The

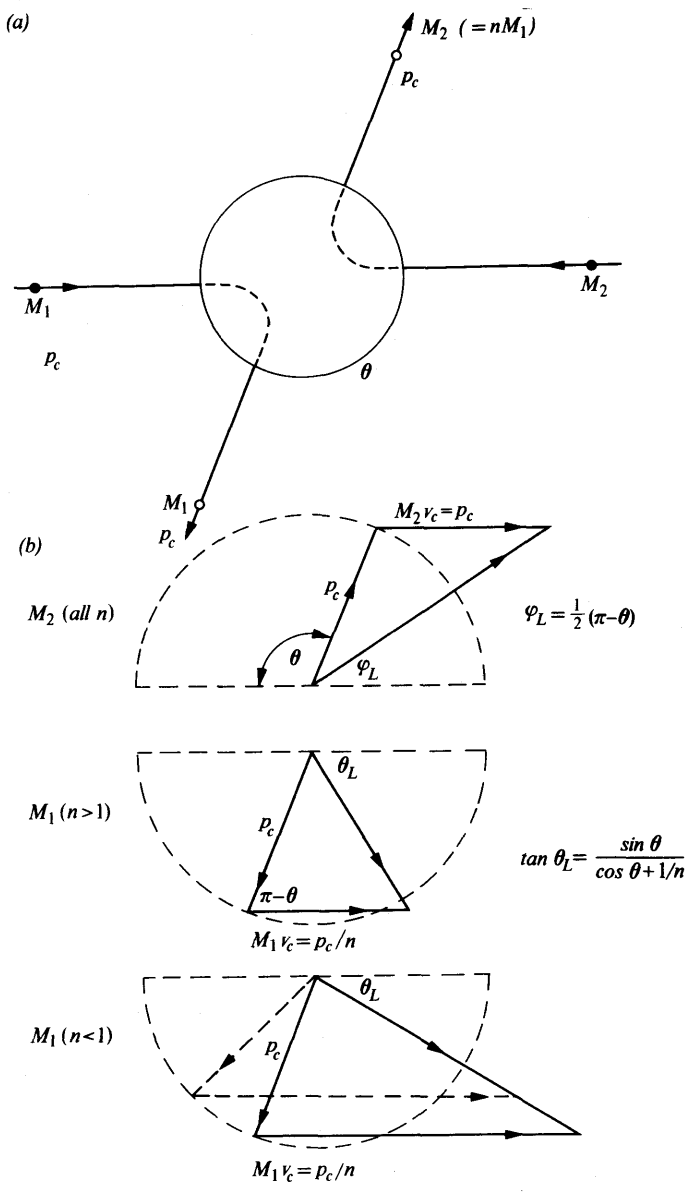

Fig. 1.4 (a) Elastic collsion between particles, c.n. system. (b) Momentum diagrams for M_1 and M_2 with n $(= M_2/M_1) >$ or < 1. These show the conversion from the c.m. system to the laboratory system. For $n < 1$ the maximum scattering angle is $\sin^{-1} n$.

diagram shows that

$$\phi_L = \tfrac{1}{2}(\pi - \theta) \tag{1.15}$$

$$\tan \theta_L = \sin \theta / (\cos \theta + (1/n)) \tag{1.16}$$

It may also be seen, by comparing the momentum diagrams for M_1, why a double-valued energy occurs for a certain range of θ_L when $n < 1$. This is found when the c.m. velocity *exceeds* that of M_1 in the c.m. system. The two energies coincide at the maximum scattering angle $\theta_L = \sin^{-1} n$ and for larger angles there is no scattering.

If the collision is *inelastic*, then in the c.m. system as well as in the laboratory the final kinetic energy will differ from its initial value by $|Q|$. This energy is distributed between the particles in such a way that their momenta are still equal and opposite. For endothermic collisions the individual c.m. momenta will be zero if the initial c.m. kinetic energy T is equal to $|Q|$. The reaction cannot take place for smaller values of T and $T_0 = |Q|$ is the *c.m. threshold energy*. The corresponding *laboratory threshold energy* T_1 is obtained by putting

$$|Q| = T_0 = \tfrac{1}{2}\mu(p_1/M_1)^2 = (\mu/M_1)T_1 \tag{1.17}$$

and is equal to the value $|Q|(M_1 + M_2)/M_2$ quoted earlier.

The relation between $|Q|$ and the laboratory threshold energy and also the existence of double-valued energies at a given angle for both of the product particles (see Ex. 1.4) are visualized more clearly by use of the c.m. system rather than the laboratory frame of reference.

1.2.4 *Relativistic processes*

As soon as kinetic energies comparable with rest energies are considered and in all cases in which calculations to the highest accuracy are necessary, relativistic kinematics must be used. In the theory of beta decay, for instance, the electron rest-energy is only 0·511 MeV and typical decay energies are about 1 MeV.

The fundamental difference between classical and relativistic kinematics is that classical definitions of linear momentum and energy lead to conservation laws that are invariant under Galilean but not Lorentz transformations. The theory of special relativity (see, for instance, Ref. 1.2*a*, Ch. 15) shows that for a particle of mass M moving with velocity v, if the linear momentum is defined as $\gamma M v$ and the energy as $\gamma M c^2$, where the Lorentz factor $\gamma = (1 - \beta^2)^{-1/2}$, $\beta = v/c$, then the corresponding conservation laws are indeed Lorentz invariant. The classical definition of momentum is the low-velocity limit of $\gamma M v$; for energy, a stationary particle has rest energy Mc^2 and a moving particle a total energy $\gamma M c^2$ so that the kinetic energy is $T = Mc^2(\gamma - 1)$. The low-velocity limit of T of course has the classical form $\frac{1}{2}Mv^2$.

It is now possible to see the physical meaning of the Q-value for an inelastic process $1+2 \rightarrow 3+4$. The energy conservation law is

$$E_1 + E_2 = E_3 + E_4 \tag{1.18}$$

and in terms of rest energies and kinetic energies this is

$$T_i + (M_1c^2 + M_2c^2) = T_f + (M_3c^2 + M_4c^2) \tag{1.19}$$

It follows by equation (1.7) that

$$[(M_1 + M_2) - (M_3 + M_4)]c^2 = T_f - T_i = Q \tag{1.20}$$

so that the Q-value is simply the difference between the initial and final masses. In nuclear reactions such as (1.8a,b) the resulting difference of kinetic energies is generally easily detected, in contrast with the *mass* difference which is small compared with either $(M_1 + M_2)$ or $(M_3 + M_4)$. In particle physics, however, energy changes are often comparable with rest energies.

In equation (1.20) M_1, M_2, M_3 and M_4 should be the masses of bare nuclei in kilograms, and Q is then in joules; conversion to the more useful MeV is straightforward. Since in reactions such as (1.8) the inclusion of the same number of electrons in the initial and final states leads to *neutral atoms* it is permissible to use atomic instead of nuclear masses in Q-value calculations. Equation (1.20) is then written

$$(M_1 + M_2) - (M_3 + M_4) = Q \tag{1.21}$$

with M_1, M_2, M_3 and M_4 in atomic mass units (a.m.u. or u) as defined in Section 6.1. These masses are tabulated, and again conversion to MeV/c^2($\propto$ MeV) or kilograms is direct. In nuclear reactions or decay processes leading to the emission of *positive* electrons, the Q-values calculated from atomic masses must be reduced by an amount $2m_ec^2$ (Sect. 6.5).

In particle physics, absolute masses are written $m_p, m_e, m_\pi, \ldots$ and are specified in kg or MeV/c^2, while momenta $p_p, p_e, p_\pi, \ldots$ are given in MeV/c. In natural units (Ref. 1.1*a*, p. 22) $c = 1$, and masses, energies and momenta are quoted in MeV or GeV. The momentum energy mass relation is then $E^2 = p^2 + m^2$.

Relativistic collision problems can be solved by the methods of Sections 1.2.1 and 1.2.2 but it is better to use the fact that energy and momentum together form a *four-vector* $p_\mu = (E, \boldsymbol{p})$. Four-vectors (Ref. 1.2*b*, Ch. 25) are quantities whose magnitude or norm is invariant under a Lorentz transformation; they have a scalar component, e.g. E, and an ordinary vector component, e.g. $\boldsymbol{p}$. Two four-vectors $A_\mu = (A_0, \boldsymbol{A})$ and $B_\mu = (B_0, \boldsymbol{B})$ have the following properties, in which a particular sign convention is adopted:

$$\left.\begin{aligned} A_\mu B_\mu &= A_0 B_0 - \boldsymbol{A} \cdot \boldsymbol{B} \\ A_\mu A_\mu &= A_0^2 - A^2 \\ A_\mu + B_\mu &= (A_0 + B_0, \boldsymbol{A} + \boldsymbol{B}) \\ (A_\mu + B_\mu) \cdot (A_\mu + B_\mu) &= (A_0 + B_0)^2 - (\boldsymbol{A} \cdot \boldsymbol{A} + \boldsymbol{B} \cdot \boldsymbol{B} + 2\boldsymbol{A} \cdot \boldsymbol{B}) \\ &= A_\mu^2 + B_\mu^2 + 2A_\mu B_\mu \end{aligned}\right\} \quad (1.22)$$

For the energy momentum four-vector the Lorentz invariant is $E^2 - p^2 = M^2$, the particle mass squared. Energy-momentum conservation implies conservation of p_μ.

For the collision problem we now have

$$p_\mu^1 + p_\mu^2 = p_\mu^3 + p_\mu^4 \quad (1.23)$$

and problems are solved by taking suitable scalar products (see Exs. 1.21–1.24). Thus, if particle 2 is at rest in the laboratory system $p_\mu^2 = (M_2, 0)$ and the $(\text{norm})^2$ for the initial system by equation (1.22) is

$$M_1^2 + M_2^2 + 2M_2 E_1 = M_i^2 + 2M_2 T_1 \quad (1.24)$$

where $M_i = M_1 + M_2$ is the total mass in the initial state. At a reaction threshold, all the final-state particles are at rest in the c.m. system and in this frame the four-momentum is $p_\mu^c = (M_f, 0)$ where $M_f = M_3 + M_4$. The $(\text{norm})^2$ for the c.m. system at threshold is M_f^2 and from equation (1.24) we find that the laboratory threshold energy is given by

$$M_i^2 + 2M_2 T_1 = M_f^2 \quad (1.25)$$

or

$$T_1 = (M_f^2 - M_i^2)/2M_2 = (M_f - M_i)(M_f + M_i)/2M_2 = |Q|(M_f + M_i)/2M_2 \quad (1.26)$$

If we put $M_f \approx M_i$ we obtain the value already noted in Section 1.2.3, i.e.

$$T_1 = |Q|(M_1 + M_2)/M_2$$

Equation (1.25) also shows that at very high energies, where $T_1 \gg M_i$, the useful energy M_f only increases as $T_1^{1/2}$, so that colliding beams with a total energy $\approx 2T_1$ offer an attractive alternative to fixed-target accelerators.

It is often necessary to transform four-vectors from one inertial frame of reference to another and the Lorentz transformation for the components of $p_\mu = (E, \boldsymbol{p})$ is

$$\left.\begin{aligned} E' &= \gamma(E - \beta p_z) \\ p'_x &= \gamma p_x \\ p'_y &= \gamma p_y \\ p'_z &= \gamma(p_z - \beta E) \end{aligned}\right\} \qquad (1.27)$$

for a velocity β of the accented system relative to the unaccented system in the positive z-direction; c is taken equal to 1. Since the transformation equations are linear they apply to the total energy $E = E_1 + E_2$ of two colliding particles and to their total momentum $\boldsymbol{p} = \boldsymbol{p}_1 + \boldsymbol{p}_2$. It then follows from equations (1.27) that the velocity of the c.m. in the laboratory system is

$$\beta_c = \boldsymbol{p}/E \qquad (1.28)$$

and the Lorentz factor for the c.m. system is then

$$\gamma_c = E/M \qquad (1.29)$$

where M is the total energy in the c.m. system.

In concluding this brief review of the high-energy collision it should perhaps be remarked that the choice of sign for the energy-momentum invariant is arbitrary and values of both $+M^2$ (as here) and $-M^2$ will be encountered. It should also be noted that the connection between mass and energy does not imply the creation or destruction of particles such as protons or neutrons, to which conservation laws apply, unless antiparticles are also involved. Energy changes in reactions relate to the energy of binding of these particles in more complex systems such as nuclei, or to the energy of formation of resonant states (Sect. 2.2).

1.2.5 *Cross-sections*

The basic probability of a nuclear reaction process is measured by finding the yield of reaction products under well-defined geometrical conditions for a known incident flux of particles or of radiation. Experimental data are reduced to *cross-sections* in the centre-of-mass system for comparison with theoretical calculations.

Consider a two-body process of the type shown in Fig. 1.1 or Fig. 1.3, namely, an elastic scattering of incident particles a (M_1) by nuclei X (M_2)

$$\mathrm{X + a \rightarrow X + a} \qquad (1.30)$$

or an inelastic process producing particles b (M_3) and Y (M_4)

$$\mathrm{X + a \rightarrow Y + b} \qquad (1.31)$$

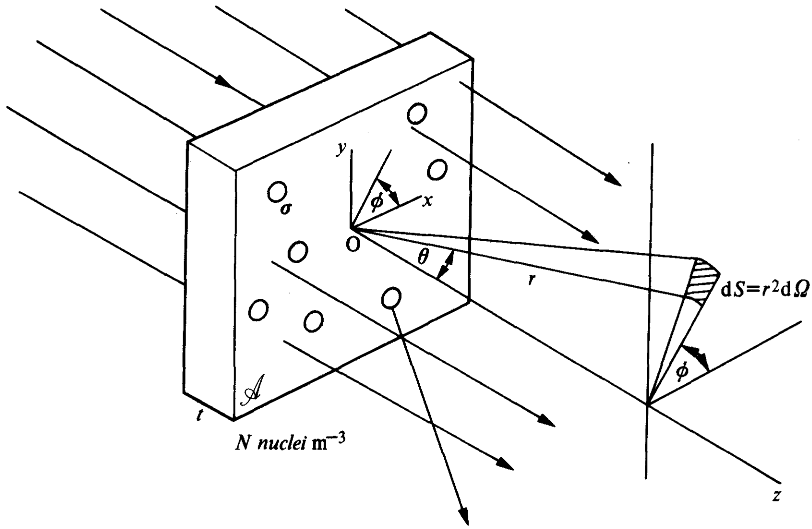

Fig. 1.5 The concept of cross-section, or collision area.

Let such a reaction take place in a target foil of thickness t and area $\mathscr{A}$ containing N target nuclei X per unit volume (Fig. 1.5) and suppose that n_i incident particles a strike the foil per second in a parallel beam, so that the incident flux Φ_i is $n_i/\mathscr{A}$. Suppose also that each target nucleus acts independently of all the others and that the beam is not significantly attenuated by the reaction processes in passing through the foil. The number of such processes that take place per second is then proportional to the number of particles incident (n_i) and to the number of target nuclei ($N\mathscr{A}t$) and may be written

$$\mathscr{Y} = n_i \,.\, (N\mathscr{A}t) \,.\, \sigma/\mathscr{A} \tag{1.32}$$

This equation defines the *cross-section* σ as an area. It is not necessarily the area of a target nucleus X, but is rather the area of the incident beam associated with each nucleus through which an incident particle has to pass if it is to cause the specified interaction. It is thus a property of both particles involved in the collision and may depend on the size of each, e.g. on the sum of their radii if the de Broglie wavelength of relative motion is small. Nuclear cross-sections are conveniently measured in *barns* ($1\text{ b} = 10^{-28}\text{ m}^2$).

Equation (1.32) may be rewritten in terms of the incident flux as

$$\mathscr{Y} = (n_i/\mathscr{A})(N\mathscr{A}t)\sigma = \Phi_i \,.\, (N\mathscr{A}t)\sigma \tag{1.33}$$

so that setting $N\mathscr{A}t = 1$, the cross-section may be defined as the yield per unit time for one target nucleus placed in unit incident flux. This particular definition is useful for theoretical comparisons because the quantity $\Phi_i\sigma$ is the probability per unit time of the process (1.30) or (1.31), and for this a general formula is provided by quantum mechanics. The expression (1.33) is also useful in practice for computing yields of radioactive elements produced by neutron activation, e.g. in a beam from a reactor; it is only necessary to know the flux, the total number of target atoms subject to this flux, and the cross-section. The yield may also be expressed as

$$\mathscr{Y} = n_i \,.\, (Nt) \,.\, \sigma \tag{1.34}$$

in which (Nt) is the number of target nuclei per unit area of the target, equal for an element to $N_A\rho_s/A$ where N_A is Avogadro's number, A is the atomic weight and ρ_s is the mass per unit area.

If only one process occurs in the target, with total cross-section σ, the actual *attenuation* of the incident beam is easily obtained by letting t become a small thickness $\mathrm{d}z$ and writing

$$-\mathrm{d}n = \mathrm{d}\mathscr{Y} = n(N\,\mathrm{d}z)\sigma$$

or

$$n = n_i \exp(-\mu z) \tag{1.35}$$

where n_i is the unattenuated number of particles, $\mu = N\sigma$ is the *linear attenuation coefficient*, sometimes also known as the *macroscopic cross-section* and z is a length. If (1.35) is rewritten

$$n = n_i \exp(-\mu z'/\rho) = n_i \exp(-\mu_m z') \tag{1.35a}$$

then $\mu_m = \mu/\rho = N_A\sigma/A$ ($\mathrm{m^2\,kg^{-1}}$) is the *mass attenuation coefficient* which is independent of the physical state of the absorber, and $z' = \rho z = \rho_s$ is a mass per unit area ($\mathrm{kg\,m^{-2}}$). The attenuation in a thin sample is

$$(n_z - n_i)/n_i = 1 - \mathrm{e}^{-\mu z} \approx \mu z \quad \text{or} \quad \mu_m z' \tag{1.36}$$

Consider now the angular dependence of the yield of reaction products a, or b. If $\mathrm{d}\mathscr{Y}$ particles are observed per unit time in the solid angle $\mathrm{d}\Omega$ defined by a detecting area $\mathrm{d}S = r^2\,\mathrm{d}\Omega$ (Figs. 1.5 and 1.9), then for one target nucleus, equation (1.33) gives

$$\mathrm{d}\mathscr{Y} = \Phi_i\,\mathrm{d}\sigma \tag{1.37}$$

and this yield constitutes a flux Φ_s of particles passing through the area $\mathrm{d}S$ at distance r from the target nucleus. We may therefore also write

$$\mathrm{d}\mathscr{Y} = \Phi_s\,\mathrm{d}S = \Phi_s r^2\,\mathrm{d}\Omega \tag{1.38}$$

and comparing equations (1.37) and (1.38)

$$d\sigma/d\Omega = r^2\Phi_s/\Phi_i \tag{1.39}$$

This quantity is conventionally called the *differential cross-section* and gives the angular distribution of the yield of reaction products with respect to the beam direction. It is numerically equal to the ratio of scattered to incident flux for one target nucleus and unit detector distance.

The differential cross-section is generally a function of the polar angles θ, ϕ (shown in Fig. 1.5) that define the detector axis and is often written $\sigma(\theta, \phi)$. The angle θ relates to the *scattering plane* defined by the direction of incidence and the direction of scattering. The angle ϕ (not that used in Sect. 1.2.1) is the azimuthal angle, between the scattering plane and a fixed reference plane, normally the zOx plane of Cartesian axes centred at O. In nuclear physics, differential cross-sections are measured in millibarns (or some other submultiple of the barn) per steradian, mb sr^{-1}.

The total cross-section for the reaction is obtained by integration of $d\sigma$, where

$$d\sigma = \sigma(\theta, \phi)\, d\Omega = \sigma(\theta, \phi) \sin\theta\, d\theta\, d\phi \tag{1.40}$$

In the case that there is no dependence of yield on the azimuthal angle ϕ, the ϕ integration gives 2π and

$$\sigma = 2\pi \int_0^\pi \sigma(\theta) \sin\theta\, d\theta \tag{1.41}$$

This cross-section is the same in the laboratory and c.m. system, since the total number of processes per second is the same. The differential cross-sections, however, are related by the equation

$$\sigma(\theta) \sin\theta\, d\theta = \sigma_L(\theta_L) \sin\theta_L\, d\theta_L \tag{1.42}$$

the azimuthal angle ϕ being the same in each system for coplanar events. Observed cross-sections are transformed to c.m. values by using equation (1.16).

The concept of cross-section is easily applied to an incident *wave system* because in practice it is necessary to collimate the incident beam and to place detectors at a distance of many wavelengths from the target nuclei. Interference between incident and scattered waves may then be neglected and asymptotic forms for radial waves may be used.

For *electromagnetic radiation*, with an incident flux of I_i joules m^{-2} s^{-1} the energy loss per second from the beam due to the target foil is written

$$I_i \,.\, (N\mathscr{A}t)\sigma \tag{1.43}$$

in direct analogy with equation (1.33). Alternatively, in analogy with equation (1.34) the loss can be expressed as

$$(I_i\mathscr{A}).(Nt)\sigma \tag{1.44}$$

in which $(I_i\mathscr{A})$ is the total energy incident per second on the scattering foil. If both the energy loss and the incident energy are divided by the photon energy $h\nu$, the flux and energy loss then relate to a number of particles as in the earlier discussion. The attenuation of a beam of gamma radiation, for instance, is then given by equation (1.35).

For the *de Broglie waves* that describe particles there is a quantum-mechanical formula for flux

$$\Phi = (\hbar/2im)(\Psi^* \operatorname{grad} \Psi - \Psi \operatorname{grad} \Psi^*)\, \mathrm{m^{-2}\, s^{-1}} \tag{1.45}$$

where Ψ is the wavefunction of a particle of mass m. For plane waves representing particles of kinetic energy T and momentum p

$$\Psi_i = A_i \exp i(kz - \omega t) \tag{1.46}$$

where k is the wavenumber, related to the particle velocity v_i by the equation

$$k = 2\pi/\lambda = 2\pi m v_i/h = p/\hbar \tag{1.47}$$

and ω is the angular frequency, given by

$$\omega = T/\hbar \tag{1.48}$$

we find

$$\Phi = (k\hbar/m)\,|\Psi|^2 = v_i\,|A_i|^2 \tag{1.49}$$

For a scattering process equation (1.39) then gives

$$v_s|A_s|^2 = v_i|A_i|^2.\,(1/r^2)\,.\,\mathrm{d}\sigma/\mathrm{d}\Omega \tag{1.50}$$

In the particular case of elastic scattering in the c.m. system we have $v_s = v_i = k\hbar/m$ at *all* angles.

1.2.6 Angular momentum

The angular distribution of a nuclear reaction process about the direction of the incident beam is intimately connected with the angular momentum transfer taking place in the process. Figure 1.6 shows a particle a approaching a fixed target nucleus X along a path which, if continued without deflection, defines an *impact parameter* b. If the linear momentum of particle a is $\boldsymbol{p}$ at a large distance from X and if $\boldsymbol{b}$ is the position vector corresponding to b, then the angular momentum of a about X is

$$\boldsymbol{L} = \boldsymbol{b} \times \boldsymbol{p} \tag{1.51}$$

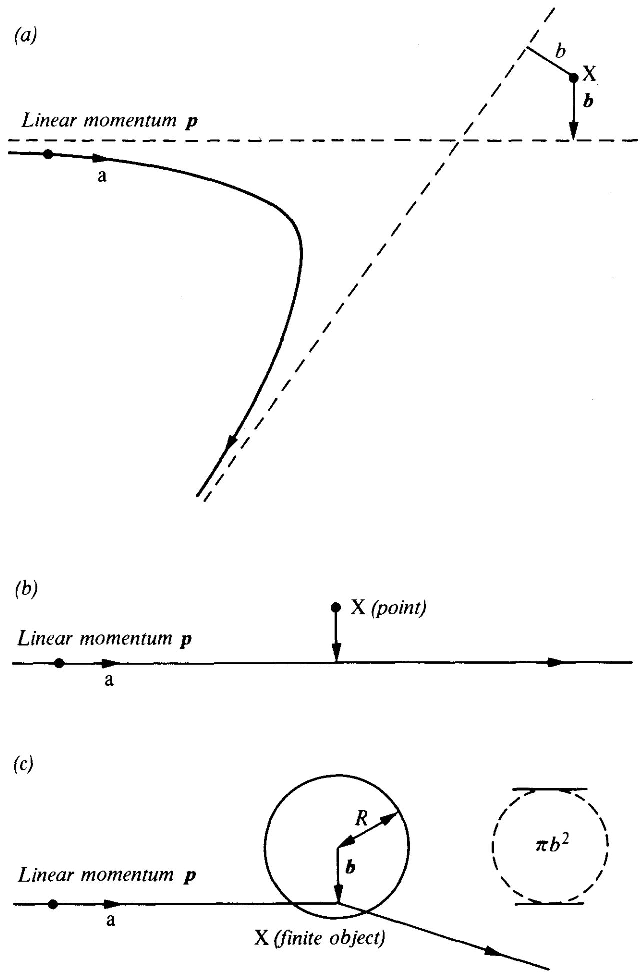

Fig. 1.6 Impact parameter $\boldsymbol{b}$ in collision of a particle a with a nucleus X. (a) Long-range force. (b) Short-range force, point nucleus. (c) Short-range force, finite nucleus, showing projected area πb^2 corresponding to collision with impact parameters 0 to b.

In the absence of external couples, and of any change of internal angular momentum, this quantity is strictly conserved in the collision so that if an elastic scattering takes place along the trajectory shown in the figure, the final direction of the scattered particle also defines a perpendicular distance b from the target X.

Kinematically $\boldsymbol{b}$ and therefore $\boldsymbol{L}$ can have any magnitude, but for an interaction to take place, a must approach close enough to X for the influence of the interparticle force to be felt. For the long-range forces of electromagnetism and gravity this can be a very large distance and in such processes (e.g. the scattering of α-particles by nuclei as illustrated in Fig. 1.6*a*, or the passage of comets near the Sun) very large angular momenta may enter the equations of motion as conserved quantities. In processes such as neutron scattering, however, in which the main force is a short-range nuclear attraction (range $\approx 10^{-15}$ m) no effect would take place for impact parameters greater than this if the target nucleus were a point object (Fig. 1.6*b*). For a finite nucleus of radius R, in which R includes the range of nuclear forces, interaction may take place for impact parameters b up to the value R, i.e. for angular momenta up to

$$\boldsymbol{L} = \boldsymbol{R} \times \boldsymbol{p} \tag{1.52}$$

but not for larger values (Fig. 1.6*c*).

If the incident particles are described by de Broglie waves, with wavenumbei and frequency as defined in equations (1.47) and (1.48), the angular momentum about the centre X is quantized. The quantum values for the total angular momentum and for its component along one of the axes are given by the equations

$$\left.\begin{aligned} |\boldsymbol{L}|^2 &= l(l+1)\hbar^2 \\ L_z &= m\hbar, \ |m| \leqslant l \end{aligned}\right\} \tag{1.53}$$

where l is the angular momentum quantum number. Frequently, a particle with $\boldsymbol{L}^2$ and L_z given by (1.53) is said to have angular momentum $l(\hbar)$, although this quantity is strictly the maximum observable component of the vector.

If the z-axis is the axis of incidence then there is no orbital angular momentum component along it, i.e. $L_z = 0$, $m = 0$. The condition (1.52) for interaction is then

$$\boldsymbol{L} \leqslant |\boldsymbol{R} \times \boldsymbol{p}|$$

or, using (1.53) and substituting for p in terms of the wavenumber k

$$\sqrt{l(l+1)}(= kb_l) \leqslant kR \tag{1.54}$$

This equation, which is often given in the form $l \leqslant kR$, limits the angular momentum transfer possible from an incident beam with given wavenumber and defines a maximum l-value $l_{\max} \approx kR$. It will be seen in Section 1.2.7 that this limitation is reflected in the degree of complexity of the angular distribution of the reaction process.

Figure 1.6*c* also shows that the cross-section for an interaction produced by incident particles with classical impact parameters uncertain by the equivalent of one unit of angular momentum cannot exceed

$$\pi(b_{l+1/2}^2 - b_{l-1/2}^2) = (\pi/k^2)[(l+\tfrac{1}{2})(l+\tfrac{3}{2}) - (l-\tfrac{1}{2})(l+\tfrac{1}{2})]$$
$$= (\pi/k^2)(2l+1) \quad \text{or} \quad \pi\lambda\!\!\!^{-2}(2l+1) \qquad (1.55)$$

This semi-classical result provides a useful limit on cross-sections.

When the target nucleus X is free to move the linear momentum of each particle with respect to the centre-of-mass is $k\hbar = \mu v_a$ where μ is the reduced mass. The total angular momentum relative to the centre-of-mass is $\mu v_a b = k\hbar b$. These quantities may be used in equations (1.51–1.55).

Angular momentum, like linear momentum and energy, is normally specified for nuclear problems in the centre-of-mass system, since the relation between external couples and rate of change of angular momentum

$$\boldsymbol{G} = \mathrm{d}\boldsymbol{L}/\mathrm{d}t \qquad (1.56)$$

is independent of the motion of the c.m.s. If $\boldsymbol{G} = 0$ then $\boldsymbol{L}$ is a constant of the motion. Such cases arise when a particle interacts with another through a purely *central* force (directed along the line of centres), and also when a charged particle moves in a plane perpendicular to the lines of force of a uniform magnetic field $\boldsymbol{B}$ (Fig. 1.7). In the latter case, for a particle of mass M and charge e, the angular momentum about an axis parallel to the lines of force and through a point O is

$$\boldsymbol{L} = \boldsymbol{r} \times M\boldsymbol{v} \qquad (1.57)$$

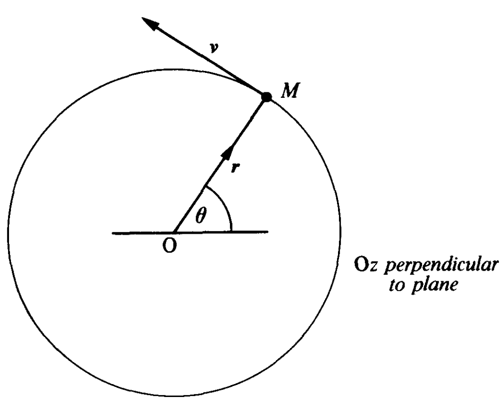

Fig. 1.7 Circular motion of a charged particle in a plane. This may be due to (*a*) a uniform magnetic field of induction $\boldsymbol{B}$ perpendicular to the plane, or (*b*) an attractive, radial force due to another particle at the centre O. In both cases the angular momentum is a constant of the motion.

and the force due to the magnetic field is

$$\boldsymbol{F} = e\,.\,\boldsymbol{v} \times \boldsymbol{B} \tag{1.58}$$

This force produces an acceleration which can be equated to the acceleration of the particle moving in a circle of centre O, and radius r with a uniform angular velocity $\omega(=v/r)$ given by

$$evB/M = \omega^2 r = v^2/r$$

or

$$\omega = eB/M \tag{1.59}$$

the so-called *cyclotron frequency* in angular measure (see Sect. 4.3.1). The angular momentum $\boldsymbol{L}$ is then also constant, as required. This is in fact an example of an axially symmetric situation, in which the strict requirement is that the *component* L_z of angular momentum along the direction of the magnetic field should be constant.

Particles and nuclei may possess an intrinsic angular momentum or *spin* $\boldsymbol{S}$ whose maximum observable z-component is $S\hbar$ where the quantum number S is integral or half-integral. For a single particle moving with respect to a centre of force with orbital angular momentum $\boldsymbol{L}$, the total angular momentum is then

$$\boldsymbol{J} = \boldsymbol{L} + \boldsymbol{S} \tag{1.60}$$

Conventionally, these symbols are used for the total electronic momenta of an atom; for a single electron within the atomic structure, or for a single nucleon in the nuclear shell model (Ch. 7), lower-case letters are used, i.e.

$$\boldsymbol{j} = \boldsymbol{l} + \boldsymbol{s} \tag{1.60a}$$

It is also conventional to use $\boldsymbol{J}$ for the spin of an elementary particle, and $\boldsymbol{I}$ for the spin of a complex nucleus, rather than $\boldsymbol{S}$. In problems in which both nuclear and electronic momenta are involved, such as hyperfine structure (Sect. 3.4), the total mechanical angular momentum of an atom is written $\boldsymbol{F}$ and

$$\boldsymbol{F} = \boldsymbol{I} + \boldsymbol{J} \tag{1.60b}$$

For a charged particle there is a magnetic moment $\boldsymbol{\mu}_l$ associated with any orbital angular momentum $\boldsymbol{L}$ because this creates a circular current, and for many particles with mass there is an intrinsic magnetic moment $\boldsymbol{\mu}_s$ associated with the spin $\boldsymbol{S}$ if this is non-zero.

If a nucleus with spin $\boldsymbol{I}$ (and $\boldsymbol{L} = 0$) is subject to a magnetic field of induction $\boldsymbol{B}$ along the z-axis (Fig. 1.8), a couple $\boldsymbol{G} = \boldsymbol{\mu}_I \times \boldsymbol{B}$ arises tending to alter the angle β between the nuclear spin axis and O. Because of conservation of angular momentum along Oz, this cannot happen, but as in the case of the electrons of an atom in the

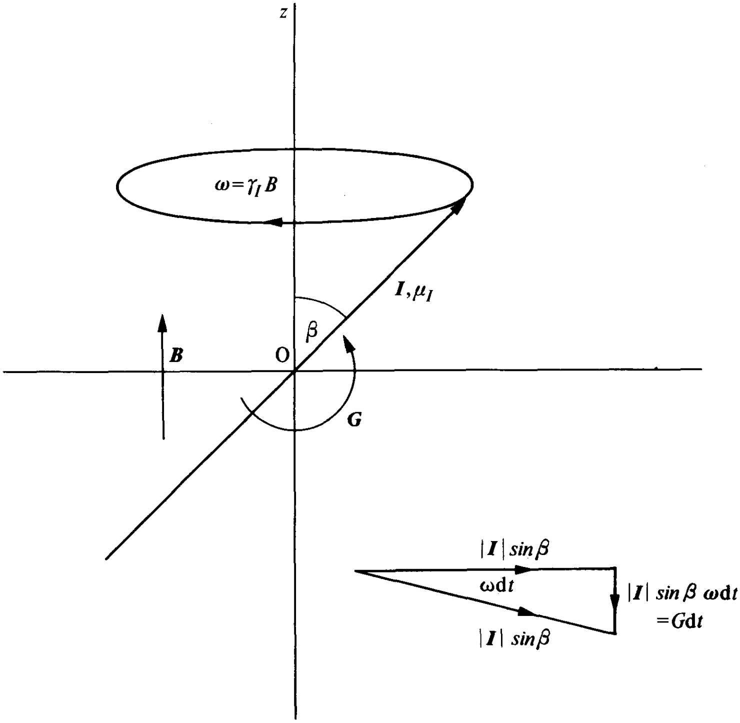

Fig. 1.8 Precession of nuclear spin $\boldsymbol{I}$ in a magnetic field $\boldsymbol{B}$. The couple is due to the interaction of $\boldsymbol{B}$ with the (positive) nuclear magnetic moment $\boldsymbol{\mu}_I$. The angular momentum created along the axis of the couple $\boldsymbol{G}$ by the precession in time dt is represented in the vector triangle.

Zeeman effect, a *precessional motion* occurs in which the z-component of $\boldsymbol{I}$ stays constant but the $\boldsymbol{I}$-vector rotates round Oz. The couple is balanced because this rotation ensures that a changing component of $\boldsymbol{I}$ continually appears along the axis of the couple. The motion is such that

$$I_z = |\boldsymbol{I}| \cos\beta = \text{constant}$$
$$\boldsymbol{G} = \boldsymbol{\mu}_I \times \boldsymbol{B} = \mathrm{d}\boldsymbol{I}/\mathrm{d}t = \boldsymbol{\omega} \times \boldsymbol{I} \tag{1.61}$$

where w is the angular velocity of the precession. This is immediately obtained as

$$\omega = (\boldsymbol{\mu}_I/\boldsymbol{I})B = \gamma_I B \tag{1.62}$$

where $\gamma_I = \boldsymbol{\mu}_I/\boldsymbol{I}$ is the *gyromagnetic ratio* for the nucleus; it is a ratio of magnetic moment to mechanical angular momentum. This precessional frequency occurs in all nuclear problems involving interactions with both static and time-varying magnetic fields.

The total energy of a particle of mass M moving about a centre of force under radial, conservative forces may be written to show the effect of conservation of angular momentum explicitly. Thus, using coordinates r and θ in the plane of motion (Fig. 1.7):

$$\begin{aligned} E &= T + V(r) \\ &= \tfrac{1}{2}M(\dot{r}^2 + r^2\dot{\theta}^2) + V(r) \\ &= \tfrac{1}{2}M\dot{r}^2 + [L^2/2Mr^2 + V(r)] \end{aligned} \tag{1.63}$$

where $L = Mr^2\dot{\theta}$ (writing $v = r\dot{\theta}$ in equation (1.57)). If then E is expressed as

$$E = \tfrac{1}{2}M\dot{r}^2 + V_{eff} \tag{1.64}$$

the new quantity V_{eff} is an effective potential energy arising partly from the centrifugal effect; it tends to prevent the close approach of the orbiting particle to the centre of force. In the quantum theory of the motion of a particle in a potential well the orbital momentum-dependent potential has an effect on the allowed energy levels of the system which varies from zero in the case of the hydrogen atom to a displacement comparable with that due to a change of principal quantum number for a nucleon in a nucleus (see Sect. 7.2).

1.2.7 Partial-wave theory

Wave theory provides a description of collisions in both nuclear and particle physics which pays particular attention to the role of the conserved quantity angular momentum. The partial-wave formalism, originated by Lord Rayleigh, is especially suitable when scattering is due to a localized spherically symmetrical potential of an extent R comparable with the reduced de Broglie wavelength $\lambda\!\!\!^{-}$ $(= 1/k)$ of the incident particle.

The formalism does not explain *why* scattering occurs; that information is contained in the interaction potential for the problem. It does, however, *describe* the scattering in terms of phase shifts which are readily determined from experimental differential cross-sections and which may be predicted according to hypotheses about the potential. The phase shifts indicate which angular momentum states are important in the scattering and their variation with c.m. energy may help to locate favoured states or resonances in the interaction, e.g. states of the compound system formed by the incident particle plus target.

The procedure is to set up the problem as a superposition of spherical wave solutions of the Schrödinger equation in the coordinates (r, θ, ϕ). If the interaction potential involves only a central force (depending only on the particle–target distance r), such solutions are eigenfunctions of the angular momentum operator and describe particles with definite $\boldsymbol{L}^2$ and L_z with respect to, say, the target as origin and a selected quantization axis Oz. For most problems the time variation of the wavefunction will disappear when particle fluxes are calculated, and it will be omitted from the beginning, so that essentially an energy-conserving steady state is

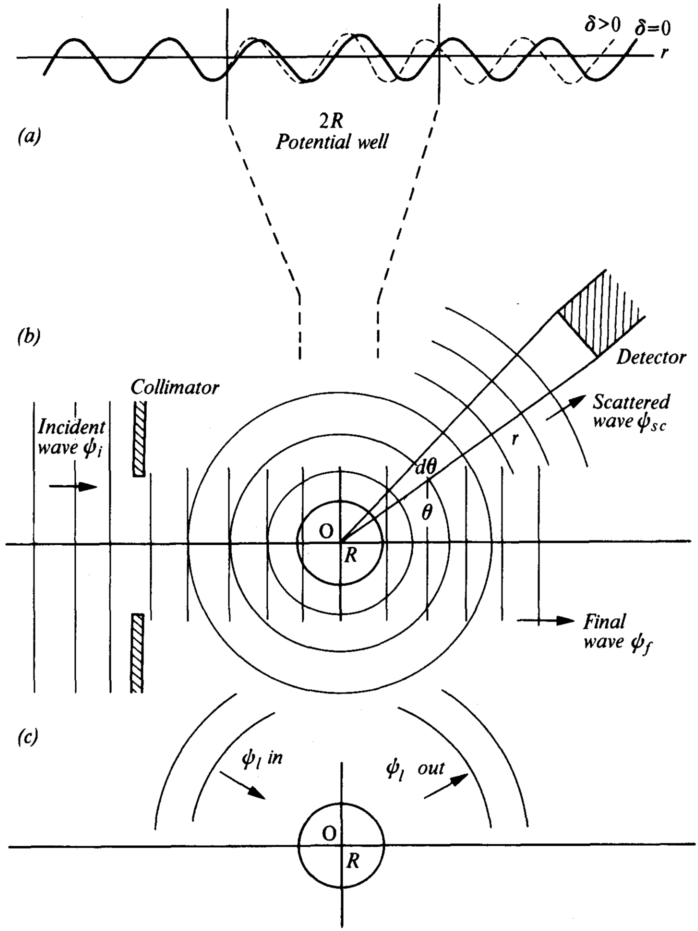

Fig. 1.9 (a) Radial de Broglie wave amplitude $r\psi$ for a free particle as a function of r showing the phase shift $\delta > 0$ produced by an attractive potential over a distance $2R$. No amplitude change is shown. For a repulsive potential a similar diagram shows that $\delta < 0$. (b) Scattering diagram (schematic) showing collimation of incident plane wave and scattered wave (not necessarily isotropic in amplitude) arising from the target nucleus. The final wave system is no longer an undisturbed plane wave. The direction Oz and the detector axis define the scattering plane, which makes an angle ϕ, not shown, with a fixed reference plane xOz. (c) Partial waves; for $l > 0$ the waves are non-isotropic.

under consideration. A particular de Broglie spherical wave amplitude as a function of r is shown in Fig. 1.9*a*; at a potential boundary there may be a change in amplitude (η) and/or a change in phase (δ). If only a phase change occurs then elastic scattering is described; an amplitude change means that inelastic processes occur.

The partial-wave formalism will be illustrated for the scattering of uncharged, spinless particles a (M_1) incident upon a spinless target nucleus X (M_2) at the origin O (Fig. 1.9*b*). The incident particles are represented by a plane de Broglie wave whose direction of propagation defines the z-axis:

$$\Psi_i = A_i \exp ikz \tag{1.65}$$

where the wavenumber k is given by equation (1.47) and the time factor $\exp(-i\omega t)$ is omitted. Strictly k and ω should refer to the c.m. system, in which

$$k = \mu v_1/\hbar \quad \text{(see eqn (1.14))} \tag{1.66}$$

where μ is the reduced mass and v_1 the laboratory velocity of the incident particles. For simplicity M_2 will be assumed infinite so that the target nucleus is fixed and the laboratory and c.m. systems are identical. The target interacts with the incident particle through a spherically symmetrical potential which may be assumed to exist within the volume of radius R shown in Fig. 1.9*b*.

The wavefunction (1.65) is an eigenfunction of the *linear* momentum operator $-i\hbar\partial/\partial z$ with eigenvalue $\hbar k = M_1 v_1$ and the flux of incident particles is given by equation (1.49) as

$$\Phi_i = (k\hbar/M_1)\,|A_i|^2 = v_1\,|A_i|^2 \tag{1.67}$$

To convert to a spherical wave representation it is first noted that the particles have no angular momentum component about the z-axis, i.e. $L_z = 0$. The angular part of the wavefunction, therefore, only involves spherical harmonics of the type $Y_l^0(\theta, \phi)$ and these may be expressed in terms of Legendre polynomials using the relation

$$Y_l^0(\theta, \phi) = [(2l+1)/4\pi]^{1/2} P_l^0(\cos\theta) = [(2l+1)/4\pi]^{1/2} P_l(\cos\theta) \tag{1.68}$$

The incident wavefunction is then written, using (r, θ) coordinates and a known expansion

$$\begin{aligned}\Psi_i &= A_i \exp(ikr\cos\theta)\\ &= A_i \sum_{l=0}^{\infty} (2l+1) i^l j_l(kr) P_l(\cos\theta)\end{aligned} \tag{1.69}$$

where $j_l(kr)$ is a *spherical Bessel function* and l is the quantum number for the orbital angular momentum about the origin, such that

$$|\boldsymbol{L}|^2 = l(l+1)\hbar^2 \tag{1.70}$$

(and $L_z = 0$ by choice of axis).

The spherical Bessel functions have a simple form in the asymptotic limit, when observations are made at a great many wavelengths distant from the scattering centre. This is, in fact, the practical case, Fig. 1.9*b*, in which the incident beam is collimated so that at the detector there is no interference with the scattered wave. The asymptotic form (valid for all kr for $l = 0$) is

$$\begin{aligned} j_l(kr) &\to \sin(kr - l\pi/2)/kr \\ &= [\exp i(kr - l\pi/2) - \exp -i(kr - l\pi/2)]/2ikr. \end{aligned} \tag{1.71}$$

in which we see two terms, corresponding when the time factor is inserted with an *outgoing and incoming partial wave* indexed by l, the angular momentum number (Fig. 1.9*c*).

If no target nucleus is present there is no scattering and the incoming and outgoing fluxes for large r obtained from equation (1.45) are identical.

If the target nucleus is present there will be some effect on the outgoing partial wave (but not on the incoming partial because of the causality principle) and the final asymptotic wave system takes the form

$$\begin{aligned} \Psi_f = A_i \sum_{l=0}^{\infty} (2l+1) i^l P_l(\cos\theta) [\eta_l \exp 2i\delta_l \exp i(kr - l\pi/2) \\ - \exp -i(kr - l\pi/2)]/2ikr \end{aligned} \tag{1.72}$$

in which η_l is the amplitude change (a real number between 0 and 1) and $2\delta_l$ is the phase difference between the outgoing partial wave with and without the scatterer present. The formula (1.45) now shows that the incoming and outgoing fluxes in the lth partial wave are not identical and the difference may be written

$$\begin{aligned} (\text{Incoming} - \text{outgoing flux, } l\text{th wave}) &\propto (k\hbar/M_1)[1 - |\eta_l \exp 2i\delta_l|^2] \\ &\propto (k\hbar/M_1)(1 - \eta_l^2) \end{aligned} \tag{1.73}$$

The wavefunction ψ_f of (1.72) describes just the elastically scattered particles, whether or not inelastic processes take place. It differs from the wavefunction ψ_i without the scatterer because the target nucleus originates a physical scattered wave of amplitude

$$\begin{aligned} \Psi_{sc} &= \Psi_f - \Psi_i \\ &= A_i \sum_{l=0}^{\infty} (2l+1) i^l P_l(\cos\theta)[(\eta_l \exp 2i\delta_l - 1) \exp i(kr - l\pi/2)]/2ikr \end{aligned}$$

by direct subtraction of equations (1.72) and (1.69), using (1.71)

$$= A_i \sum_{l=0}^{\infty} (2l+1)P_l(\cos\theta)[\eta_l \exp 2i\delta_l - 1]\exp ikr/2ikr \quad (1.74)$$

(using the identity $i^l = \exp il\pi/2$)

$$= A_i f(\theta) \exp(ikr)/r \quad (1.75)$$

where $f(\theta)$ is a length known as the *scattering amplitude.* The existence of a scattered wave implies removal of particles from the direct beam, and from the definition (1.39) we may immediately obtain the differential cross-section $d\sigma_{el}(\theta)/d\Omega$. The necessary quantities are

$$\begin{aligned} \text{incident flux} &= k\hbar/M_1 \,.\, |A_i|^2 \\ \text{scattered flux} &= k\hbar/M_1 \,.\, |A_i|^2\, |f(\theta)|^2/r^2 \end{aligned} \quad (1.76)$$

whence

$$d\sigma_{el}/d\Omega = |f(\theta)|^2$$

Often, and especially in particle physics, it is useful to write

$$f(\theta) = 1/k \sum_{l=0}^{\infty} (2l+1)P_l(\cos\theta) f_l \quad (1.77)$$

where

$$f_l = (\eta_l \exp(2i\delta_l) - 1)/2i \quad (1.78)$$

is a complex quantity known as the *partial-wave amplitude.* The integrated cross-section for elastic scattering is then

$$\sigma_{el} = \int d\sigma_{el} = \int 2\pi\, |f(\theta)|^2 \sin\theta\, d\theta$$

$$= (1/k^2) \sum (2l+1)^2 \,.\, 4\pi/(2l+1) \,.\, |f_l|^2$$

using the orthogonality and conventional normalization of the Legendre polynomials. It follows that

$$\sigma_{el} = \sum \sigma_{el}^l = (4\pi/k^2) \sum (2l+1)\, |f_l|^2$$

$$= (\pi/k^2) \sum (2l+1)[1 + \eta_l^2 - 2\eta_l \cos 2\delta_l] \quad (1.79)$$

where σ_{el}^l is the integrated cross-section for the lth partial wave.

We now consider the particular cases of zero and finite inelastic scattering, and some general results.

(i) *No inelastic processes* (elastic scattering only). If elastic scattering is the only process that takes place in the interaction, there is no absorption and $\eta_l = 1$ for all partial waves. From (1.79) the cross-section then takes the simpler form

$$\sigma_{el} = (4\pi/k^2) \sum_{l=0}^{\infty} (2l+1) \sin^2 \delta_l \tag{1.80}$$

Substitution of $\eta_l = 1$ into the asymptotic forms of the final wave (1.72) and scattered wave (1.74) shows that δ_l is the phase shift of the lth component of these waves, whereas the phase shift of the outgoing *partial* wave is $2\delta_l$ (eqn (1.72)).
(ii) *Finite inelastic scattering.* When non-elastic processes occur, the corresponding outgoing particles have a different velocity and perhaps a different nature from the incident beam and ψ_{sc} cannot be obtained in the form (1.74). The integrated cross-section for all such processes, however, may be obtained from equation (1.73) and definition (1.39). Integrating over the whole solid angle using the normalization of $P_l(\cos\theta)$ and summing the partial-wave series we obtain

$$\sigma_{inel} = (\pi/k^2) \sum (2l+1)(1-\eta_l^2) \tag{1.81}$$

In this case, both elastic and inelastic processes occur together and the total removal of particles from the beam is represented by

$$\begin{aligned}\sigma_{total} &= \sigma_{el} + \sigma_{inel}\\ &= (\pi/k^2) \sum (2l+1)[2 - 2\eta_l \cos 2\delta_l]\end{aligned} \tag{1.82}$$

(iii) *Limiting cross-sections.* The cross-sections (1.79), (1.81) and (1.82) are expressed as the incoherent sum of partial cross-sections corresponding to particles incident upon the scattering centre with angular momentum component $l\hbar$, i.e. with a classical impact parameter $l\hbar/p_1 = l/k$. Such particles will interact with the target nucleus if $l/k < R$, the nuclear dimension. If they so interact, the maximum cross-sections that may be observed are seen to be

$$\left.\begin{aligned}\sigma_{el}^l &= (4\pi/k^2)(2l+1)\\ \sigma_{inel}^l &= (\pi/k^2)(2l+1)\\ \sigma_{total}^l &= (4\pi/k^2)(2l+1)\end{aligned}\right\} \tag{1.83}$$

The elastic cross-section reaches its maximum (resonance) value when $\eta_l = 1$ and $\delta_l = \pi/2$ and the inelastic cross-section then vanishes. The inelastic cross-section reaches its maximum value, which is exactly that given in equation (1.55) as a result of semi-classical considerations, when $\eta_l = 0$, corresponding to complete absorption of the outgoing partial wave; the elastic cross-section then has the same value and the total cross-section is $(2\pi/k^2)(2l+1)$. It is also clear from equations (1.79) and (1.81) that although elastic scattering may take place without absorption ($\eta_l = 1$) the converse is not true. An absorption process in which particles of orbital angular momentum $l\hbar$ are removed creates an elastic scattering, known as *shadow scattering* with an angular distribution characteristic of l.

The angular distribution of elastic scattering, in the present case in which Coulomb forces are neglected, is given by equation (1.76). From the formulae for P_l (cos θ) (Appendix 1) it can be seen that if the maximum l-value entering into the scattering for spinless particles is L then the angular distribution contains powers of cos θ up to $\cos^{2L}\theta$ only.

(iv) *Phase shifts and the scattering potential.* Within the radial extent of the force between the incident particle and target nucleus, an interaction potential must be added to the Schrödinger equation describing the elastic scattering. For an attractive potential the kinetic energy within the range of the force is increased and the deBroglie wavelength decreases. Figure 1.9*a* shows that this means a positive phase shift δ_l in the asymptotic wave. Conversely, a repulsive potential gives a negative phase shift.

The partial-wave analysis so far outlined must be modified if a Coulomb potential is involved in the scattering, since this is of long range and affects waves with all l-values. The modified analysis shows that a calculable term α_l representing the Coulomb phase shift appears in the elastic scattering amplitude together with the nuclear phase shift δ_l.

(v) *An example of phase-shift analysis.* A practical case is shown in the work of Clark *et al.* (Fig. 1.10) on the elastic scattering of

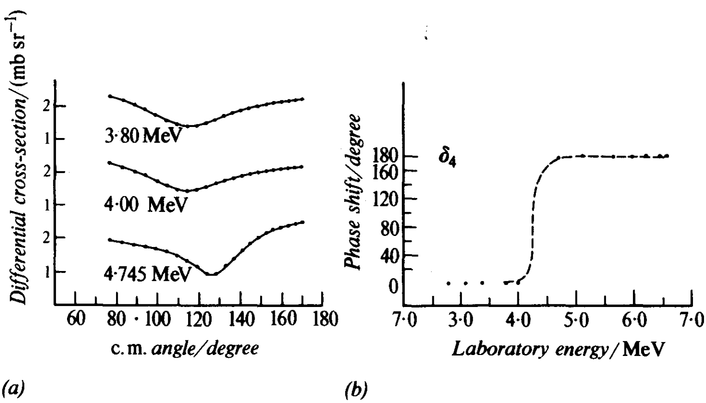

Fig. 1.10 Partial-wave analysis, $^{12}C(\alpha,\alpha)^{12}C$. (*a*) Differential cross-sections near 4·0 MeV bombarding energy. (*b*) The $l = 4$ phase-shift energy variation. (From Clark, G. J. *et al.*, Nuclear Physics, **A110**, 481, 1968.)

α-particles by ^{12}C:

$$^{12}C+\alpha \rightarrow {}^{16}O^* \rightarrow {}^{12}C+\alpha \tag{1.84}$$

Differential cross-sections were obtained over the c.m. angular range 70–170° for laboratory energies 2·8 MeV to 6·6 MeV and were analysed by the use of equations (1.76)–(1.78) with $\eta_l = 1$ and with the inclusion of Coulomb scattering terms to take account of the nuclear charge. Figure 1.10*a* shows the differential scattering cross-section for energies near to 4·00 MeV and Fig. 1.10*b* gives the variation of the $l=4$ phase shift with energy. This phase shift passes through 90° at an energy of about 4·3 MeV, and indicates a level of spin 4 and even parity at an excitation energy of 10·36 MeV in the intermediate nucleus $^{16}O^*$ in process (1.84).

Another well known and simple example of phase shift analysis is a study of the $\Delta(1236)\pi^+$-proton scattering resonance, as described by Perkins (Ref. 1.1*a*, p. 272) and shown in Fig. 2.10. In this and the preceding case of $^{12}C(\alpha, \alpha)^{12}C$, one partial wave only is dominant and inelastic processes are negligible. The partial-wave method is generally useful in sorting out complex situations in which overlapping resonances are present, and measurements of both elastic and inelastic (or total) cross-sections as a function of energy are necessary.

1.3 Conservation laws and constants of motion

In the preceding sections, and indeed in the whole of classical physics, the principles of conservation of total energy, of linear and of angular momentum have been assumed for macroscopic systems not acted on by external forces or couples. In atomic and nuclear physics we assume that the same principles apply, albeit that they should be expressed in quantum mechanical language. In these domains, however, other plausibly conserved quantities such as parity and isobaric spin have appeared. The discovery of the non-conservation of these quantities in the weak interaction has led to a deeper examination of the meaning of conservation laws in physics and their relation to the basic forces of nature.

In classical mechanics it is possible to formulate Newton's laws of motion in terms of the Hamiltonian function H giving the total energy ($H=T+V$) of a system of n interacting particles, and the position coordinates q_i and momentum values p_i of individual particles. The equations of motion are then

$$\left.\begin{aligned} \dot{q}_i &= \partial H/\partial p_i \\ \dot{p}_i &= \partial H/\partial q_i \end{aligned}\right\} \quad \text{for} \quad i=1 \text{ to } n \tag{1.85}$$

Suppose now that a small and equal change is made to all the position coordinates so that q_i becomes $q_i + \Delta q$. The change in the total energy is then

$$\begin{aligned}\Delta H &= \Delta q(\partial H/\partial q_1 + \partial H/\partial q_2 + \cdots) \\ &= \Delta q(\dot{p}_1 + \dot{p}_2 + \cdots)\end{aligned} \tag{1.86}$$

If, however, linear momentum is a constant of the motion the sum $\sum \dot{p}_i$ vanishes and $\Delta H = 0$ so that the Hamiltonian is unchanged by, or *invariant* to, the spatial displacement Δq. Conversely, one may postulate that if the Hamiltonian is invariant to a particular transformation (e.g. Δq) then the associated (or conjugate) mechanical quantity (e.g. p) is a *constant of the motion.*

This is so far simply a re-statement of what is already understood as a consequence of Newton's third law of motion. But the idea of invariance under transformations is a new and important one because it underlines the existence of symmetry in natural phenomena. A simple geometrical example is given in Fig. 1.11; the rotation of an equilateral triangle through 120° about a central axis perpendicular to its plane reproduces the original figure. This shape is invariant to the 120° rotation, or in other words, there is three-fold symmetry in the pattern.

These ideas can be immediately transferred to a system which must be described by quantum mechanics. There will then be a state wave function Ψ which is in general a linear combination of normalized eigenfunctions of the Hamiltonian operator H. The expectation (or average) values of observable quantities D are obtained by applying suitable operators to Ψ and integrating over configuration space, e.g.

$$\langle D \rangle = \int \Psi^* D \Psi \, \mathrm{d}^3 r \tag{1.87}$$

gives the expectation value of quantities such as position, kinetic energy, momentum.

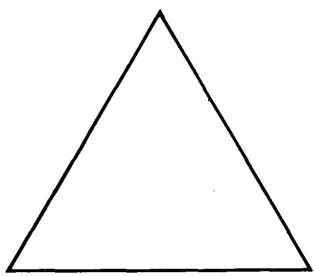

Fig. 1.11 The equilateral triangle has a three-fold axis of symmetry.

The effect of a transformation may be assessed by enquiring whether or not the expectation value of such an operator depends on time, i.e. whether or not it is a constant of the motion. To do this it is convenient to use the Heisenberg, rather than the Schrödinger formulation of quantum mechanics, because this uses time-independent state functions and gives an explicit formula for the time dependence of an operator D, namely

$$dD/dt = i/\hbar[HD - DH] = i/\hbar[H, D] \tag{1.88}$$

where the bracketed quantity is called the *commutator* of the operator D with the Hamiltonian or total energy operator H. If D is a constant of the motion then the commutator vanishes, i.e. $DH = HD$, which means as an operator equation, that the Hamiltonian is unaffected by, or invariant to, the D operation.

If now D represents space translation, as in the foregoing classical example, then for an infinitesimal displacement

$$D = 1 + \Delta x \,.\, \partial/\partial x \tag{1.89}$$

But quantum mechanics relates the gradient operator directly to the x-component of linear momentum by the equation

$$p_x = -i\hbar\frac{\partial}{\partial x} \tag{1.90}$$

and conservation of linear momentum follows. A conservation law is thus connected with the invariance of the Hamiltonian under the appropriate transformation or, in equivalent terms, to the fact that the operator for this transformation commutes with the Hamiltonian.

In Table 1.1a the transformations corresponding with the classically familiar conserved quantities are listed. These quantities are as

TABLE 1.1

Conserved quantity	*Transformation*
(a) Linear momentum p	Space translation Δx
Angular momentum L	Space rotation $\Delta\phi$
Total energy E	Time translation Δt
Mass M^2	Lorentz transformation (Δr, Δt)
(b) Parity π	Space inversion P
Isobaric spin T	Rotation in isospin space $T_x + iT_y$
Charge parity π_c	Particle–antiparticle conversion C
(no quantum number)	Time reversal T
(c) Charge Q	
Baryon number B	Gauge transformations
Lepton number L	Gauge transformations
Strangeness S	Gauge transformations
Charm C	Gauge transformations

far as one knows at present rigorously conserved in quantum mechanical systems and for all interactions, subject only to the relaxation permitted by the uncertainty relations:

$$\Delta p_x \,.\, \Delta x \approx \hbar, \qquad \Delta L_\phi \,.\, \Delta\phi \approx \hbar, \qquad \Delta E \,.\, \Delta t \approx \hbar \tag{1.91}$$

In Table 1.1*b* are listed some of the quantities used in nuclear physics that are not universally conserved, but may nevertheless provide useful quantum numbers for certain classes of process, especially those governed by the strong nuclear interaction. It will be noted that parity and charge parity relate to discontinuous transformations of the nature of mirror-reflection processes. Isobaric spin is discussed in Section 5.6.

Finally, in Table 1.1*c* are noted the important particle numbers, including charge, which can be brought into the general framework of the present discussion in terms of a special type of transformation which just adds a phase factor to the corresponding particle wave-functions. Baryons and leptons are defined in Section 2.3; for strangeness and charm see Sections 2.2.2/3.

The conservation laws discussed in this section lead directly to the *selection rules* that determine which quantum states of a nuclear system may be connected by a specific operation, e.g. the emission of a quantum of electric dipole radiation or of a particle carrying total angular momentum J.

1.4 The spherically symmetrical potential well

Angular momentum plays an essential role, not only in the dynamics of collision processes in which both attractive and repulsive forces may appear, but also in determining the order of the energy levels of a particle bound within an attractive potential well. This is really a special case of the general formalism already discussed for scattering problems, namely that the system 'particle plus target' has a negative total energy. The zero of the energy scale is taken to be the state of the system when the particle is removed to an infinite distance from the centre of the potential well. As it moves in under an attractive force, its kinetic energy increases and its potential energy diminishes, but the total energy remains zero. Finally, in the process of binding some energy is released, usually as radiation, and the total energy becomes negative. Both the scattering and the bound-state problems are described by the Schrödinger equation and solutions for the bound states in simple wells are given in Reference 1.3. Only a very brief treatment will be presented here.

Let the interaction between particles M_1 and M_2 be described by a spherically symmetrical potential $V(r)$ and suppose that M_2 is very large so that c.m. motion may be disregarded. In such a field (Ref. 1.3 and Sect. 1.2.7) solutions of the wave equation may be sought that are simultaneous eigenfunctions of the Hamiltonian or total energy operator and of the operators $\boldsymbol{L}^2$ and L_z for angular momentum. These eigenfunctions have the form

$$\Psi_{nlm} = R_{nlm}(r) Y_l^m(\theta, \phi)$$

where $Y_l^m(\theta, \phi)$ is a spherical harmonic and $R_{nlm}(r)$ is a radial function; the index n will be defined later and the polar coordinates used are shown in Fig. 1.12. The eigenvalues for the angular momentum operators are given, as in Section 1.2.6, by the equations

$$\left.\begin{aligned} \boldsymbol{L}^2\Psi_{nlm} &= l(l+1)\hbar^2\Psi_{nlm}, \qquad & l &= 0, 1, 2, \ldots \\ L_z\Psi_{nlm} &= m\hbar\Psi_{nlm}, & |m| &\leq l \end{aligned}\right\} \tag{1.92}$$

where l is the orbital angular momentum quantum number and m is the magnetic quantum number. Following spectroscopic convention, states with $l = 0, 1, 2, 3, 4, \ldots$ are known as s-, p-, d-, f-, g-, ... states.

The orbital motion, as noted in Section 1.2.6, adds a repulsive centrifugal potential to the radial wave equation so that the motion takes place in an effective potential

$$V_{eff} = V(r) + l(l+1)\hbar^2/2Mr^2 \tag{1.93}$$

The one-dimensional radial wave equation, which remains after removal of the angular part of the Schrödinger equation, is then

$$\left[-\frac{\hbar^2}{2M}\frac{1}{r^2}\frac{\mathrm{d}}{\mathrm{d}r}\left(r^2\frac{\mathrm{d}}{\mathrm{d}r}\right) + l(l+1)\frac{\hbar^2}{2Mr^2} + V(r)\right]R(r) = ER(r) \tag{1.94}$$

where E is the total energy of the particle of mass M ($= M_1$). This

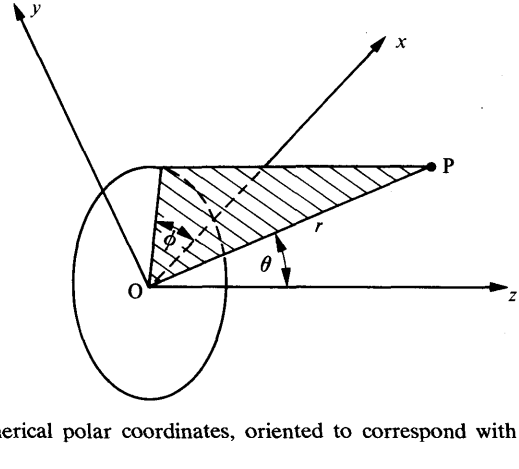

Fig. 1.12 Spherical polar coordinates, oriented to correspond with the scattering problem.

equation is simplified by the substitution

$$u(r) = rR(r) \tag{1.95}$$

and then becomes

$$\frac{d^2u}{dr^2} + \frac{2M}{\hbar^2}\left[E - V(r) - l(l+1)\frac{\hbar^2}{2Mr^2}\right]u = 0 \tag{1.96}$$

Solution of this equation for discrete eigenfunctions u_{nl} and energy eigenvalues E_{nl} is equivalent to fitting appropriate waves to the effective potential V_{eff}, remembering that when the coefficient of u_{nl} becomes negative the wavenumber becomes imaginary. The energy E_{nl} in an eigenstate is determined by the depth of the effective potential well and by the number of wavelengths within it, so that the states are characterized by two suffixes, l and n. Although there are $(2l+1)$ eigenfunctions ψ_{nlm} for each l, corresponding with the permitted m-values, these are degenerate, i.e. they all have the same energy because in the absence of external fields the direction of the z-axis is arbitrary. The *orbital angular momentum* quantum number l determines not only the effective well shape for a given $V(r)$ but also the *parity* of the orbital motion as $(-1)^l$ where $+1$ means even and -1 odd parity. It counts the number of angular nodes in the wavefunction Ψ_{nlm} as θ varies from 0 to π.

The suffix n could be the number of radial nodes, or changes in sign, in the function $u(r)$ or $R(r)$ as r varied from 0 to infinity. It would then be the *radial quantum number* n_r ($\geqslant 0$), and this usage is appropriate to the short-range potentials of nuclear physics. More generally, however, n is the *principal quantum number*, equal to $n_r + l + 1$ ($\geqslant 1$), which is the total number of nodes or changes of sign in both radial and angular eigenfunctions plus 1; for a given principal quantum number n we have $l \leqslant (n-1)$. This definition of n is useful for long-range potentials.

Further progress requires specification of the form of the potential $V(r)$ and it will be useful to consider the Coulomb potential and the oscillator potential, representing respectively forces of a long-range and a short-range character.

1.4.1 *The Coulomb potential*

If

$$V(r) = -Ze^2/4\pi\varepsilon_0 r \tag{1.97}$$

and if the particle is an electron ($M = m_e$), we have the case of a hydrogen-like atom which is fully discussed in Reference 1.3 in which diagrams of the effective potential and radial eigenfunctions (known as associated Laguerre polynomials) are to be found. The energy eigenvalues are

$$E_{nl} = -\tfrac{1}{2} \,.\, 1/(n_r + l + 1)^2 \,.\, Z^2e^2/4\pi\varepsilon_0 a_0 = -(1/2n^2)Z^2e^2/4\pi\varepsilon_0 a_0 \tag{1.98}$$

where a_0 is the Bohr radius $4\pi\varepsilon_0\hbar^2/m_e e^2 = 5{\cdot}29 \times 10^{-11} m$ and $n = 1, 2, 3, \ldots$.

For a given principal quantum number the energy does not depend on l, a degeneracy that arises from the special shape of the Coulomb potential. The sequence of hydrogen-like levels shows a decreasing spacing as the dissociation energy $E = 0$ is approached.

In terms of the quantum numbers n_r, l the levels of the electron in this field are

$$(n_r, l) \equiv (0, 0); \qquad (1, 0), (0, 1); \qquad (2, 0), (1, 1), (0, 2)$$

or in terms of n, l

$$(n, l) \equiv (1, 0); \qquad (2, 0), (2, 1); \qquad (3, 0), (3, 1), (3, 2)$$

$$\text{i.e.} \quad 1s \;; \qquad 2s \;, 2p \;; \qquad 3s \;, 3p \;, 3d$$

The hydrogen-like degeneracy of these atomic levels with respect to l is removed when the central field departs from a Coulomb shape. For the *screened* Coulomb shape, in which the potential decreases towards $r = 0$ relatively more rapidly than in the pure Coulomb field, the wavefunctions with low l-values, which tend to exist closer to the central and deeper part of the potential, are bound relatively more tightly than those with larger l for the same principal quantum number. The sequence of levels then becomes, in the (n, l) scheme

$$1s; \quad 2s; \quad 2p; \quad 3s; \quad 3p; \quad 3d; \ldots$$

but a general dominance of the central charge still persists in the sense that levels of a given principal quantum number remain close together and the main energy displacement occurs with change of n.

In a hydrogen-like atom these states may be occupied by the single electron of the atom and they are connected by radiative transitions. In the structure of more complex atoms the hydrogen-like states provide basic levels for occupation and are filled by electrons in accordance with the Pauli principle which permits two electrons (with opposite spin) for each quantum state (n, l, m). It follows that for a principal quantum number (n) the corresponding *shell* contains $2n^2$ electrons.

1.4.2 The oscillator potential

If

$$V(r) = -U + \tfrac{1}{2}M\omega^2 r^2 \tag{1.99}$$

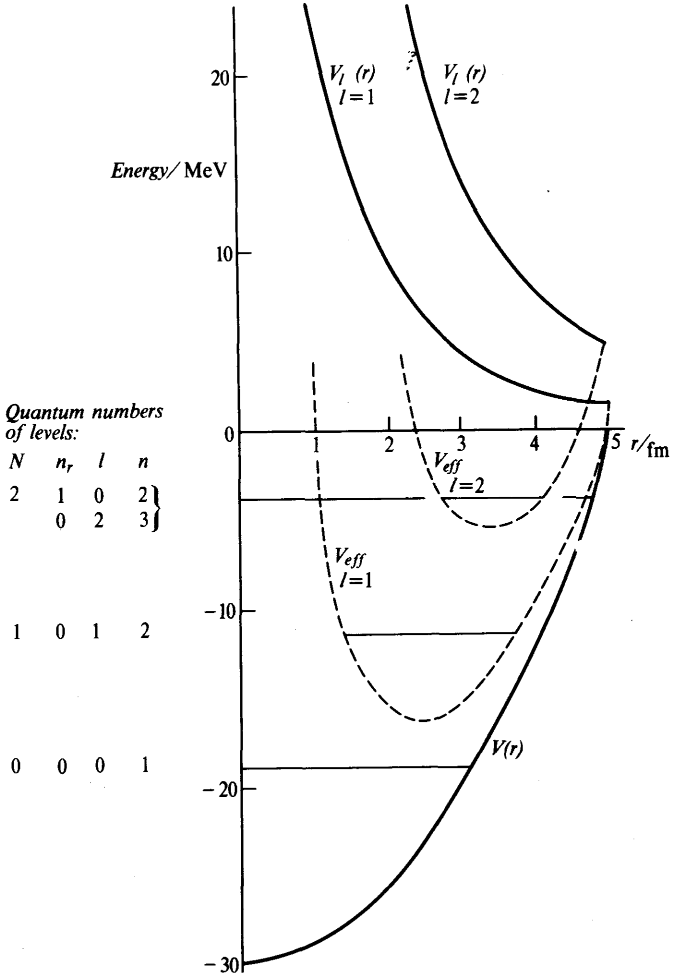

Fig. 1.13 An oscillator potential drawn with $V(r)=(-30+1{\cdot}2r^2)$ MeV for $0<r<R$ where $R=5$ fm and with $V(r)=0$ for $r>R$. Centrifugal potentials $V_l(r)$ are drawn for the case $V_l=20{\cdot}5l(l+1)/r^2$ MeV corresponding with a proton moving in the well. Levels of the effective potential (dotted) are shown, with quantum numbers.

the motion of the particle of mass M is that of a three-dimensional harmonic oscillator of angular frequency ω.

The potential well is shown in Fig. 1.13 together with centrifugal potentials $V_l(r)$ for $l=1$ and 2. The well may be regarded as a short-range potential for nuclear physics if the value of r corresponding with $V(r)=0$ is comparable with the size of an average nucleus. The radial eigenfunctions for the oscillator are also associated Laguerre polynomials, or Hermite polynomials if Cartesian coordinates are used. For a one-dimensional oscillator it is well known that the energy levels, measured from the bottom of the well, are at excitations

$$E'_n = (n + \tfrac{1}{2})\hbar\omega \qquad n = 0, 1, 2 \cdots \tag{1.100}$$

and in the three-dimensional case

$$E'_{n_1 n_2 n_3} = (n_1 + n_2 + n_3 + \tfrac{3}{2})\hbar\omega = (N + \tfrac{3}{2})\hbar\omega \tag{1.101}$$

where $N = n_1 + n_2 + n_3$ ($\geqslant 0$) is the oscillator quantum number. This gives the sequence of equally spaced levels shown in Fig. 1.13. In contrast with the case of the Coulomb potential, the oscillator levels do not close up as the dissociation energy is approached.

For each value N a range of values of the radial quantum number n_r and of the orbital momentum number l is possible, such that

$$N = 2n_r + l \tag{1.102}$$

There is thus a degeneracy with respect to l since, for example, for $N = 2$ both s-states (with $n_r = 1$) and d-states (with $n_r = 0$) have the same energy. This degeneracy may be removed if the well is distorted from the pure simple-harmonic shape. The level order is then

$$(n_r, l) \equiv (0, 0); (0, 1); (1, 0); (0, 2); (1, 1); (0, 3)$$

or in terms of (n, l)

$$(n, l) \equiv (1, 0); (2, 1); (2, 0); (3, 2); (3, 1); (4, 3)$$

i.e. 1s ; 2p ; 2s ; 3d ; 3p ; 4f

It will be noted from Fig. 1.13 that, in further contrast with the levels of the long-range potential, the effect of changes of n_r and of l on the energy is similar for the oscillator. Moreover, the effect of the well shape on the level order is opposite to that of the screened Coulomb potential. For the same principal quantum number ($n = n_r + l + 1$), states of high l-value are found to be more strongly bound than those of lower l. This is because the hydrogen-like degeneracy is removed, but the well has no singularity at the origin, so that the s-states are less strongly disturbed.

The number of fermions, e.g. electrons, protons or neutrons, that may be accommodated in the levels corresponding with oscillator quantum number N is $(N+1)(N+2)$, allowing for two possible spin directions for each spatial state (n, l, m). The oscillator states, re-ordered by the addition of spin-orbit coupling, provide a set of basic levels for nuclear shell model calculations (Ch. 7).

1.5 Summary

This introductory chapter reviews some of the kinematic relations used in the description of nuclear collisions and sets up the formal definition of cross-section, which is one of the main experimental observables for such collisions. The role of angular momentum in the wave mechanical theory of scattering is examined, and shown to provide a link with the sequence of energy levels for a particle moving in a central potential well.

Examples 1

Sections 1.2.1–1.2.3

1.1* Prove the formula (1.6) given in the text.

1.2 For the collision of Fig. 1.1, show that conservation of momentum leads to the relation

$$p_1/q = \sin(\theta_L + \phi_L)/\sin\theta_L$$

and hence, using equation (1.6) obtain the relation

$$M_1/M_2 = \sin(2\phi_L + \theta_L)/\sin\theta_L$$

(This expression was used in early track-chamber studies for identifying the masses of colliding particles).

1.3* Deduce equation (1.11).

1.4* By inspection of equation (1.11) show that the condition for observing a single group of particles M_3 at any given angle θ_{3L} is that

$$Q + T_1 \geqslant M_1 T_1/M_4$$

Show also that when this condition is not fulfilled there is a maximum value $\theta_{3\max}$ at which particles of mass M_3 can be seen, given by

$$\cos^2\theta_{3\max} = [(M_3+M_4)/M_1M_3][(M_1-M_4)-M_4Q/T_1]$$

and that for all $\theta_3 < \theta_{3\max}$ the energy is double-valued. Show further that these two expressions include the conditions already stated for the case of elastic scattering ($Q=0$).

1.5 From the last expression in Example 1.4, deduce that when Q is negative, the threshold energy for production of particles $M_3 + M_4$ is

$$T_1 = |Q|\,(M_1+M_2)/M_2$$

(Assume that $(M_3+M_4)=(M_1+M_2)$. Note that at threshold the product particles are at rest in the c.m. system).

1.6 Show that in elastic scattering with $n>1$ the minimum energy T_1' of the scattered particle is $T_1[(M_1-M_2)/(M_1+M_2)]^2$. Show also that when $n<1$ the energy of the scattered particle at the greatest possible scattering angle is $T_1(M_1-M_2)/(M_1+M_2)$.

1.7 An α-particle ($M_1=4$) is scattered through an angle of 56° by collision with a heavier nucleus, which is observed to move off at an angle of 54° with the original direction of the α-particle. Find the probable mass number of the struck nucleus. [≈12]

1.8 By use of Fig. 1.4 or otherwise, verify that for elastic scattering the momentum transfer to M_2 is the same in both laboratory and c.m. systems.

1.9 The scattering of neutrons by protons may be regarded as a collision between equal particles each of mass 1 (in a.m.u.). Show that the laboratory angle of scattering of the neutron θ_L is half the corresponding c.m. angle θ. Compute the angle through which deuterons (mass 2 a.m.u.) are scattered by protons for c.m. angles of 30°, 45°, 90° and 135°.

1.10 For the inelastic collision of Fig. 1.3 show that for M_3 the angle θ_{3L} is determined by equation (1.16) but with n given by

$$n^2 = (T+Q)/T \,.\, M_2M_4/M_1M_3 \quad \text{where} \quad T = \tfrac{1}{2}\mu(p_1/m_1)^2$$

(Note that n is the ratio of the velocity of M_3 in the c.m.s. to the velocity of the c.m.s. in the laboratory).

1.11* Draw a momentum diagram for particle M_3 in the inelastic collision of Fig. 1.3. If the angle and energy of this particle in the laboratory system are T_L, θ_L and in the c.m.s. system T and θ, show that

$$T = T_L + a - 2\sqrt{T_L a}\cos\theta_L$$

and

$$T_L = T + a + 2\sqrt{Ta}\cos\theta$$

where

$$a = \tfrac{1}{2}M_3 v_c^2$$

Show also that $\sin\theta_L/\sin\theta = (T/T_L)^{1/2}$.

1.12 The reaction ^{38}Ar(p, n)^{38}K$^{\mathrm{m}}$ has a Q-value of $-6{\cdot}824$ MeV. Find the energy of the bombarding protons at the threshold for the production of ^{38}K$^{\mathrm{m}}$ using integral masses (Ar$=$K$=38$, n$=$p$=1$). What is the c.m. energy of the neutrons for a proton energy of 10 MeV? For this proton energy write a programme that tabulates θ_L and T_L for θ from 0 to 135° in 5° intervals. Use the formulae given in Example 1.11 or equation (1.11). [2·84 MeV]

Section 1.2.4

1.13* A particle of mass m and velocity β collides with a stationary particle of mass M. Show that the velocity of the c.m. system is

$$\beta_c = \beta\gamma m/(M+\gamma m)$$

and that the Lorentz factor of this system is

$$\gamma_c = (M+\gamma m)/E_c$$

where E_c is the total energy of the two particles in the c.m. system.

Evaluate E_c in terms of M, m and γ and show that when $M=m$, $\gamma_c = [(1+\gamma)/2]^{1/2}$.

1.14 Two particles of mass M each travelling with speed β approach head-on. Show that the total energy of one in the rest frame of the other is $M(1+\beta^2)/(1-\beta^2)$.

1.15 Neutral mesons (π°) are produced by the reaction pp$\rightarrow$ppπ°. Show that the threshold proton kinetic energy is $(m_\pi^2/2m_p + 2m_\pi)$.

1.16 By using energy and momentum transformations show that if a particle moves at an angle θ_L with the z-axis in the laboratory frame, the corresponding angle θ' in a system moving with speed β in the positive z-direction is given by

$$\tan\theta_L = \sin\theta'/\gamma(\cos\theta' + \beta/\beta')$$

where β' gives the velocity of the particle in the second system. Compare this result with the non-relativistic equation (1.16).

1.17 For an energy above threshold in the reaction $1+2\rightarrow3+4$ show that the energy of particle 3 in the c.m. system is

$$E_{3c} = (E^2 + M_3^2 - M_4^2)/2E$$

(Use $E = E_{3c} + E_{4c}$ and $p_{3c} = p_{4c}$.)

1.18 Calculate the total energy and momentum of an electron which has been accelerated through a potential difference of 0·511 MeV. What are its Lorentz factor and its β-value? [2,$\sqrt{\frac{3}{4}}$]

1.19 What is the laboratory kinetic energy of the incident pion that just forms the baryon resonance Δ(1236 MeV) when incident on a proton? (Take $m_\pi =$ 139 MeV, $m_p = 938$ MeV.) [196 MeV]

1.20* Find the momentum transfer $|\boldsymbol{q}|$ in the following processes, expressing your result in units of $\hbar$, i.e. as an inverse length:
(*a*) the scattering of electrons of energy 100 MeV through a laboratory angle of 25° by a heavy nucleus. [0·22 fm^{-1}]
(*b*) the scattering of 65 MeV α-particles by an ^{16}O nucleus if the recoil nucleus is projected at a laboratory angle of 60°. [2·84 fm^{-1}]

1.21* A particle of mass M collides elastically with a stationary particle of equal mass. After the collision the angle between the trajectories of the two particles is ψ, and their kinetic energies are T_1' and T_2. Show that:

$$\cos\psi = [(1+2M/T_1')(1+2M/T_2)]^{-1/2}$$

Comment on the important differences between this relation and the classical one and show that it reduces to the latter when T_1' and T_2 are both much less than M.

Calculate ψ when the particles are nucleons, the kinetic energy of each one after the collision being 2 GeV. [60°]

1.22 In the collision described in the previous example, the projectile particle is scattered through an angle θ. Show that its kinetic energy, T_1', after the collision is:

$$T_1' = T_1\cos^2\theta/[1+T_1\sin^2\theta/2M]$$

where T_1 is its initial kinetic energy. Compare this result with the classical one.

1.23 A Λ-hyperon decays at rest into the two particles proton (p) and negative pion (π). If the energy release in the decay is Q, show that the ratio of the kinetic energies of the two decay particles is

$$(Q+2m_p)/(Q+2m_\pi)$$

Find the individual kinetic energies, given that $m_\Lambda = 1116$ MeV, $m_p =$ 938 MeV, $m_\pi = 139$ MeV. [$T_p = 5{\cdot}5$ MeV, $T_\pi = 33{\cdot}5$ MeV]

1.24 If the Δ particle in Example 1.23 decayed while it was moving with a velocity $\beta = 0{\cdot}5$, what would be the laboratory angles of the decay products for a centre-of-mass angle of 90°? (Use the result given in Ex. 1.16) (p, 10·5°; π, 45°]

1.25* The reaction ^{34}S(p, n)^{34}Cl has a threshold at a proton energy of 6·45 MeV. Calculate (non-relativistically) the threshold for the production of ^{34}Cl by bombarding a hydrogenous target with ^{34}S ions. For the (p, n) reaction, use equation (1.26) to investigate the nature of the relativistic correction necessary in deducing an accurate Q-value. [219·3 MeV]

Section 1.2.5

1.26 Calculate the de Broglie wavelength of
(*a*) an electron of energy 1 MeV; [$8{\cdot}8\times10^{-13}$m]
(*b*) a proton of energy 1000 MeV; [$7{\cdot}3\times10^{-16}$m]
(*c*) a nitrogen nucleus of energy 140 MeV. [$6{\cdot}5\times10^{-16}$m]

1.27 Show that the differential cross-section $\sigma_L(\theta_L)$ for the scattering of protons by protons in the laboratory system is related to the corresponding quantity in the c.m. system by $\sigma_L(\theta_L) = 4\cos\theta_L\sigma(\theta)$.

1.28 The cross-section for the reaction $^{10}B+n \rightarrow {^7Li}+{^4He}$ is 4×10^3 barn at a certain energy and it is the only reaction that takes place. Calculate the fraction of a ^{10}B layer that disappears in a year in a flux of neutrons of $10^{15}\,m^{-2}\,s^{-1}$. [0·013]

1.29 A finely collimated beam of α-particles having a current of 1 μA bombards a metal foil (thickness 2 g m^{-2}) of a material of atomic weight 107·8. A detector of area $10^{-4}\,m^2$ is placed at a distance of 0·1 m from the foil so that the α-particles strike it normally on the average and counts at a rate of 6×10^4 particles s^{-1}. Calculate the differential cross-section for the scattering process at the angle of observation, neglecting c.m. corrections. [1·72 b sr^{-1}]

Section 1.2.6

1.30 Show that the relativistic form of equation (1.59) for the cyclotron frequency is

$$\omega = eB/\gamma M \quad \text{where} \quad \gamma=(1-\beta^2)^{-1/2},\ \beta=v/c.$$

1.31 Calculate the perpendicular distance of the line of flight of a 10-MeV proton from the centre of a nucleus when it has an orbital momentum, with respect to this point, of $3\hbar$. Calculate also the distance for a photon of energy 5 MeV and angular momentum $\hbar$. [$4{\cdot}3\times10^{-15}$ m, $3{\cdot}9\times10^{-14}$ m]

1.32 The impact parameter for Rutherford scattering by a fixed charge Z_2e is given by

$$b=(Z_1Z_2e^2/4\pi\varepsilon_0M_1v_1^2)\cot\theta/2$$

where the symbols have their usual meaning. Calculate the angular momentum quantum number l of a 1 MeV proton with respect to the scattering centre ($Z_2=90$) for an angular deflection of 90°. [14]

1.33* Particles of mass m_1 (charge $-e$) and mass m_2 (charge $+e$) describe circular orbits around their centre of mass with angular velocity ω under their mutual interaction. Calculate the total angular momentum and magnetic moment of the system. If the angular momentum is quantized, show how the magnetic moment is related to the Bohr magneton μ_B.

Section 1.2.7

1.34* Show that the energy distribution of protons projected from a thin hydrogenous target by a homogeneous beam of neutrons is uniform up to the maximum available energy T_0 providing that the interaction involves only s-waves.

1.35 By comparing the expressions (1.77) and (1.82) for $f(\theta)$ and σ_{total} prove the relation:
Imaginary part of $f(\theta)$ for $\theta=0°=k\sigma_{total}/4\pi$. This is known as the *optical theorem*, because it relates the scattered wave to the total disturbance of the incident wave as in the case of optical refraction.

1.36* Show that if a scattering centre is a perfect absorber for all particles with a classical impact parameter up to R (black disc) then

$$\sigma_{el}=\sigma_{inel}=\pi(R+\lambda\!\!\!^{-})^2$$

1.37* At the surface of an impenetrable sphere of radius R the de Broglie wave amplitude must vanish. Use equation (1.72) to deduce the corresponding s-wave phase shift, and calculate the differential and integrated elastic cross-section in the case $\lambda\!\!\!^{-} \gg R$.

Compare the latter with the result obtained classically by integrating over all impact parameters for the elastic scattering of a point object by a hard sphere.

'Hard-sphere' scattering is often a good approximation to represent background scattering effects in nuclear processes.

1.38 Write a programme that tabulates σ_{el}, σ_{inel} and σ_{total} as a function of η_l for intervals of η_l of 0·05 between the values 0 and 1. Display the results graphically and check the maximum values noted in equation (1.83).

1.39 Calculate the s-wave phase shift for the elastic scattering of a particle of mass M and kinetic energy T scattered by a square well of depth U_0 and radius R. [$\tan\delta = (k/k')\tan k'R - \tan kR$]

1.40 The measured integrated elastic scattering cross-section for a beam of 1-MeV neutrons incident on a certain heavy target is $2\times10^{-28}\ \mathrm{m}^2$. On the assumption that there are no inelastic processes calculate the corresponding phase shifts: (a) for pure s-wave, (b) for pure p-wave, and (c) for pure d-wave. How could these cases be distinguished? [63°, 31°, 23°]

Section 1.4

1.41* The radial eigenfunctions for a particle of mass M moving in a spherically symmetrical square well potential of radius R and infinite depth are of the form $(1/\sqrt{Kr})J_{l+1/2}(Kr)$ where l is the angular momentum quantum number and K is the internal wavenumber.

Assuming that $J_{1/2}(x) \propto \sin x$, and $J_{3/2}(x) \propto \sin x/x - \cos x$, determine the relative order of the first three s- and p-states (use a computer programme for $J_{3/2}$).

1.42* By using equation (1.102) and summing over m-values, prove the statement that $(N+1)(N+2)$ nucleons may be accommodated in the levels with oscillator number N.

1.43* The energy levels for the oscillator potential cannot be found by the method of Example 1.41 because the potential does not suddenly become infinite. They are obtained by solving the wave equation in a series, as for the hydrogen atom.

Determine the minimum value of the effective potential for the motion in which the angular momentum quantum number is l.

1.44* Consider a square-well potential of depth V and radius R, such that the $3p$ level is just bound. Using the eigenvalues for an infinite well (see Example 1.41) show that this level is also just bound in other square-well potentials with the same value of VR^2. If the $3p$ level is observed as an (unbound) scattering resonance in the interaction of protons of energy 6·2 MeV with a target of $^{117}\mathrm{Sn}$, estimate the well depth and also the energy at which a similar resonance might be seen for a target of $^{124}\mathrm{Sn}$. Assume that the nuclear radius is $R = 1{\cdot}25A^{1/3}$ fm.